Al-Farouk journal of sciences
Volume (2), Issue (3) (JUNE, 2026)
ISSN: 3135-2359

مجلة الفاروق للعلوم
المجلد (2) ملحق العدد 3 يونيو 2026
ردمد: 3135-2359

Improving Operational Resilience and Peak-Load Management in the Al-Ruwais Network Through Coordinated PV, Battery Storage, and Demand Response

Marwan K. Al-Mashakwi
University of Zawiya, Faculty of Natural Resources, Department of Renewable Energy, Zawiya, Libya
Email: m.almashkawi@zu.edu.ly
ORCID: 0009-0004-9667-7370

Osama Mohammed Abdalrhman
University of Zawiya, Faculty of Engineering, Department of Electrical and Electronic Engineering, Zawiya, Libya
Email: o.abdulrahman@zu.edu.ly
ORCID: 0009-0002-8759-5299

This article is extracted and developed from the 2025 Ph.D. research proposal entitled "Enhancing Electrical Network Resilience through Advanced Load Demand Management, Including Load Forecasting with Renewable Energy Integration in West Libya," submitted to the Libyan Academy for Postgraduate Studies. [1]

تاريخ الاستلام: 2026/05/30 تاريخ المراجعة 20/06/ 2026 تاريخ القبول:2026/06/28- تاريخ النشر27/07/ 2026

Abstract

High-voltage networks in western Libya operate under a demanding combination of pronounced daily and seasonal load variation, incomplete station-level visibility, and narrow security margins whenever a transformer or feeder is unavailable. The engineering challenge is therefore broader than forecasting accuracy. A statistically acceptable forecast can still lead to overload, voltage stress, uneven feeder loading, or emergency shedding when it is not translated into a feasible operating action. The same principle applies to photovoltaic generation (PV) can reduce daytime imports, yet an uncoordinated plant may leave the evening peak almost unchanged and can simply relocate stress within the network for these reasons, we conducted a study of a mini-loop represented by the **Al-Ruwais** loop in the western Libya network.

This research is considered an extension of the doctoral dissertation. introduces the Hybrid Neural Forecasting Resilience Oriented Load Management (HNF-ROLM) framework for Libya's Al-Ruwais network, using (GECOL) demand data. It integrates an (FNN) forecast with a decision algorithm coordinating (PV, BESS, DR), and reinforcement under normal and (N-1) constraints. Performance is evaluated via (ENS, SAIDI, SAIFI), and a Resilience Index (RI), moving beyond mere forecasting accuracy MATLAB software was used. Results show (PV) cuts daytime imports, while (BESS) and (DR) provide critical evening-peak and contingency support, their coordinated use significantly reduces unserved energy, outage duration/frequency, and network violations while improving (RI). The planning layer identifies when demand growth requires structural reinforcement confirming that operational flexibility and firm upgrades are complementary. HNF-ROLM strengthens resilience via PV, BESS, and DR, delivering peak relief while guiding staged reinforcement planning for future security.

Keywords: *Hybrid Neural Forecasting-Resilience-Oriented Load Management (HNF-ROLM), General Electricity Company of Libya (GECOL), forward Neural Network (FNN), photovoltaic (PV), Battery Energy Storage System (BESS), Demand Response (DR), Energy Not Supplied (ENS), System Average Interruption Duration Index (SAIDI), System Average Interruption Frequency Index (SAIFI), Resilience Index (RI),*

1. INTRODUCTION

The operating challenge in western Libya is often labelled a load-forecasting problem. In practice, a control engineer faces a coupled forecasting-and-coordination problem: the forecast indicates what is likely to occur, the network model determines whether the expected power can be transferred safely, and the operating policy decides how PV, storage, demand response, switching, or controlled shedding should be used as the margin narrows. Keeping these stages separate can produce a prediction that looks accurate on paper but offers little help in the control room.

Forecast evaluation must preserve chronology, disclose the forecasting horizon, report complementary error measures, and examine the hours that matter most to operation. Mean Absolute Error (MAE) describes the usual error magnitude, Root Mean Square Error (RMSE) gives greater weight to large misses, and Mean Absolute Percentage Error photovoltaic (MAPE) supports comparison across demand scales. None of these indicators, however, states how much service is ultimately lost after an incorrect or stressed decision. The present study therefore extends the evaluation chain to (ENS, SAIDI, SAIFI, and RI). [2]

The empirical DATA upon which this study is built is deliberately constrained in scope, favoring a focused and well-curated dataset over a sprawling collection of disparate measurements. Specifically, it draws upon 456 hourly field observations, meticulously recorded and compiled from 19 distinct operational reports issued by the national utility authority GECOL. This modest yet carefully selected sample size is not a limitation but a conscious methodological choice; it dictates the adoption of a compact Feedforward Neural Network (FFNN) architecture, which is significantly more defensible and statistically robust in this context than an unnecessarily deep or intricate learning model that would invariably be prone to overfitting and poor generalization when applied to unseen operational conditions [3].

This article is a focused outcome of the 2025 doctoral proposal rather than a substitute for the complete thesis programme. The proposal sets the broader objective of strengthening electrical-network resilience through advanced demand management, load forecasting, and renewable-energy integration in West Libya. The present paper narrows that objective to Al-Ruwais, makes the forecast-to-decision link explicit, and tests whether service can be preserved during normal operation, forecast error, PV reduction, feeder derating, transformer N-1 conditions, official holidays, seasonal stress, and a blackout scenario.

The contribution is fivefold: measured GECOL load characterization; a transparent transfer of the learned regional load shape to the disclosed Al-Ruwais asset envelope; a standardized hourly projection from 2027 to 2036; coordinated PV+BESS+DR and reinforcement screening through HNF-ROLM; and two auditable software implementations. MATLAB is the primary implementation required for the study, while Python provides an independently executable verification path.

1.1 Focused Research Context

Recent comparative forecasting work confirms that model choice should be driven by data quality, horizon, and operational purpose rather than by complexity alone. Prophet, gradient-boosting, and deep-network approaches can each be useful, but their value depends on disciplined validation and on how the prediction is used. [4]

Reviews of electricity-load forecasting likewise show that preprocessing, feature design, chronology, and reproducibility are often as important as the selected machine-learning architecture. This supports the compact and transparent network adopted here. [5]

Accurate forecasting also has consequences beyond a smaller statistical error: it reduces reserve uncertainty and supports more stable scheduling and market or dispatch decisions. The Al-Ruwais study carries this principle forward by measuring the service consequence of the action. [6]

Hybrid recurrent and attention-based models can capture complex short-term temporal behaviour when continuous, high-quality datasets are available. Their performance establishes a useful future benchmark, although the present 456-hour evidence base does not justify such a large architecture. [7]

Long-term demand forecasts are most valuable when they are connected to strategic investment timing. This is the role of the ten-year HNF-ROLM loop, which converts annual growth into explicit capacity and resilience triggers. [8]

Mid-term ensemble methods demonstrate the benefit of combining complementary representations of trend, variability, and uncertainty. HNF-ROLM applies the same hybrid philosophy at a system level by coupling a neural predictor with a constraint-aware operating layer. [9]

Joint treatment of electricity consumption and local generation is increasingly important in networks with distributed energy resources. The present formulation follows that direction by forecasting demand while explicitly coordinating PV, storage, and responsive load. [10]

2. MEASURED GECOL OPERATING DATA

The source dataset was obtained from operating reports issued by the Western Region of the General Electricity Company of Libya. Retained fields include regional demand, total system demand, available generation, system frequency, and hourly load shedding. The 19 reports contribute 456 hourly values distributed across the months of 2023. Table 1 summarizes the disclosed monthly samples, while Figures 1 and 2 reveal the daily shapes and seasonal variation. [11]

Their value lies in capturing real behaviour, but they do not represent every temperature extreme, switching state, outage sequence, holiday, or social event. The study therefore uses them to learn a regional shape and demonstrate a reproducible workflow. The MATLAB and Python programs import the same deterministic 456-hour demonstration set from the published monthly minimum, average, maximum, and sample-day counts. This fallback verifies the software path and must not be cited as a replacement for the measurements.

Table 1. Measured sample summary by month from the 2023 GECOL reports

Month	Sample days	Minimum MW	Average MW	Maximum MW
1	2	3047	3937.7	4719
2	2	3943	4934.4	5650
3	2	2734	3773.8	4498
4	2	2334	3152.5	4123
5	2	2513	3202.2	4022
6	1	2845	3455.8	3926
7	2	4775	5427.3	5886
8	1	5258	5909.4	6313
9	1	4207	5076.0	5636
10	1	3045	3909.0	4651
11	2	2869	3871.5	4743
12	1	2642	3296.7	4082

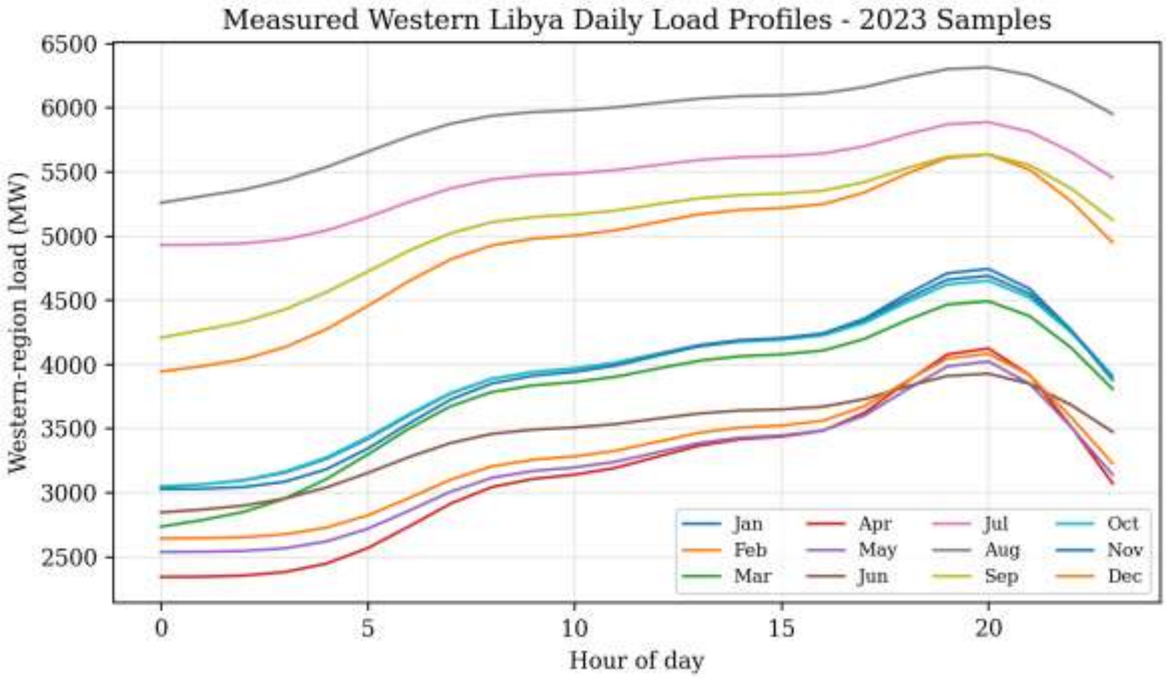

Fig. 1. Measured Western Libya daily load profiles in the available 2023 samples.

The spread between daily curves shows why one average day is insufficient. Hour-of-day and month must remain explicit inputs to the forecast.

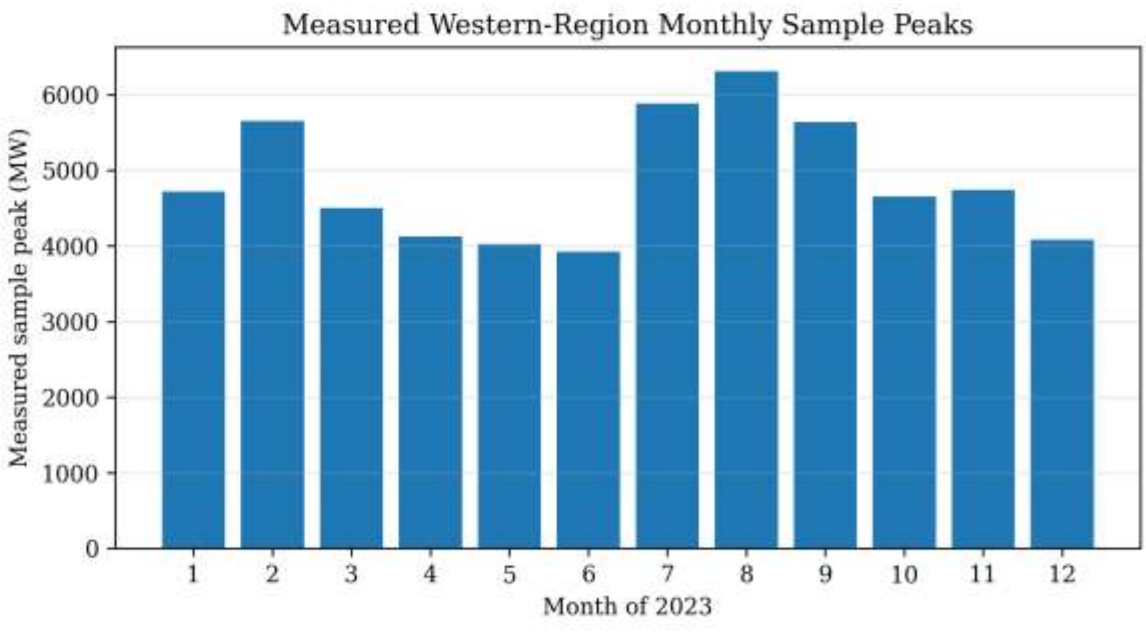

Fig. 2. Measured monthly sample peaks; the highest available observation occurs in August.

August contains the highest available sample peak. Summer operating plans should therefore pre-position storage and reserve before the evening ramp.

2.1 Al-Ruwais Network Asset Data

The available one-line diagram identifies the Al-Ruwais 220-kV station, two 220/66-kV transformers rated 63 MVA each, and associated 66/11-kV load points serving Nalut, Tiji, Jadu, Zintan, Shakshuk, Rehibat, Cement Nalut, PS3, PS4, and neighbouring areas. Transformer ratings, nominal voltages, named load points, and diagram distances are treated as source asset data. Conductor impedance, verified ampacity, transformer taps, protection settings, switching status, customer counts, and coincident power factor remain essential field-data requirements. [12]

Table 2. Source data and planning assumptions used in the capacity screen

Item	Calculation or assumption	Value
220/66-kV source transformers	2 × 63 MVA	126 MVA
Planning power factor	Declared screening value	0.90
Equivalent active-power capability	126 × 0.90	113.400 MW
One-transformer N-1 capability	63 × 0.90	56.700 MW
2026 planning peak	80% of normal capability	90.720 MW
Central annual growth	Compound planning assumption	8%
Planning horizon	Ten standardized non-leap years	2027-2036

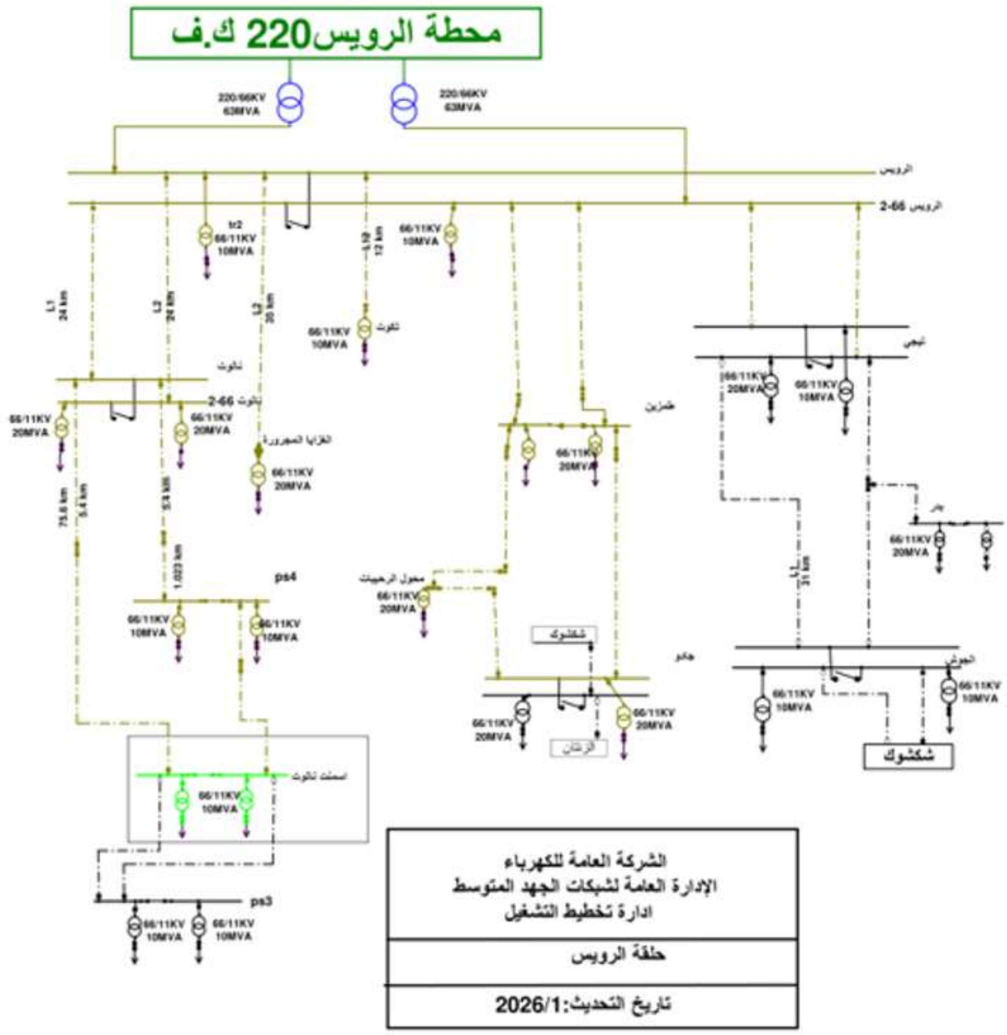

Fig. 3. Real Al-Ruwais 220-kV station and associated 66-kV network one-line diagram, updated January 2026. Source: supplied Al-Ruwais study file.

The one-line diagram establishes topology, nominal voltages, ratings, and distances; design approval still requires verified impedances, ampacities, taps, switching, and protection data.

Table 3. Load-point ratings and distances transcribed from the Al-Ruwais diagram

Load point	Installed MVA	Distance km
Nalut	40	24.0
Nalut-2	40	48.0
Tiji	20	31.0
Takut	10	66.0
Badr	20	70.0
Al-Ghazaia	20	43.0
Jadu	20	35.0
Zintan	40	47.0
Shakshuk	40	70.0
Rehibat	10	59.0
Cement Nalut	20	75.6
PS3	20	76.6
PS4	20	75.6

2.2 PV, BESS, DR, and Planning Assumptions

The source study retains a PV module record with 239.7 W rated power, 30.65 V and 7.82 A at maximum power, 37.08 V open-circuit voltage, 8.33 A short-circuit current, and 14.9% efficiency. A 30-MWp plant and an annual specific yield of 1850 kWh/kWp are planning assumptions rather than procurement values. The final design must replace them with an approved module and inverter datasheet, measured irradiance, temperature coefficients, dust and soiling losses, reactive-power capability, and interconnection requirements. [13]

High PV penetration also changes voltage-control, fault-response, and stability requirements. For that reason, the planning profile used in this paper is separated from final inverter-control and protection studies; a procurement decision should not be made from energy yield alone. [14]

The BESS and DR values are also scenario parameters. They were chosen to make the dispatch logic visible and to test whether a practical amount of short-duration flexibility can protect service. HNF-ROLM keeps every assumption in a single configuration block so that GECOL or another researcher can change a value without rewriting the algorithm. The equivalent 63-MVA reinforcement block is not a construction approval; it represents any verified combination of transformer capacity, feeder transfer, network reconfiguration, or firm local support that produces the same active-power transfer effect. [15]

Table 4. PV, BESS, DR, and resilience-planning assumptions

Parameter	Value	Status or purpose
PV module power	239.7 W	From supplied study file
PV plant rating	30 MWp	Planning scenario
Specific yield	1850 kWh/kWp-year	Planning scenario
BESS power / energy	20 MW / 100 MWh	Firm flexibility screen
BESS round-trip efficiency	90%	Planning scenario
BESS operating SOC range	10%-90%	Intertemporal constraint
Demand-response power	15 MW	Controllable-load screen
DR daily energy limit	60 MWh/day	Comfort/process constraint
RI planning trigger	0.85	Study-specific threshold
Reinforcement block	63 MVA equivalent	Transfer-capability surrogate

3. SYSTEM MODELING

The Al-Ruwais case is represented as a chronological quasi-static planning model. At each hour t and planning year y, the external inputs are forecast demand, available PV power, equipment availability, calendar context, and the selected disturbance. Controllable quantities are BESS charging and discharging, DR activation, PV curtailment where permitted, verified transfer, reinforcement status, and controlled load shedding. The calculated electrical state includes source loading, feeder loading, bus-voltage magnitude, current, losses, and BESS state of charge.

With both 63-MVA transformers available, the installed apparent-power rating is 126 MVA. At the declared planning power factor, this corresponds to a 113.4-MW active-power screen. A first-order N-1 event removes one transformer and reduces the source screen to 56.7 MW. These values are necessary capacity checks, not a complete security proof: thermal ratings, reactive demand, voltage criteria, tap positions, feeder ampacity, topology, protection, and stability must also be satisfied. [16]

3.1 Source and Ten-Year Load Formulation

(1) Total Apparent-Power Rating of the Source Transformers

$$S_{\text{source}} = N_T \cdot S_T \quad (1)$$

- S_{source}: The total apparent-power nameplate rating of the aggregate source transformer bank, measured in MVA.
- N_T: The number of source transformers whose ratings are being summed (for the initial two-unit arrangement, $N_T = 2$).
- S_T: The nameplate apparent-power rating of a single transformer, measured in MVA.

Equation (1) adds the nameplate ratings of the available source transformers. For the initial two-unit arrangement it gives 126 MVA. This is the starting capacity envelope; it does not by itself prove acceptable feeder loading or contingency performance.

(2) Conversion of MVA Rating to Active-Power Capability for Planning

$$P_{\text{source}} = S_{\text{source}} \times PF \quad (2)$$

- P_{source}: The resulting active-power capability (in MW) derived from the conversion, which is the quantity used by the neural forecasting model.

- S_{source}: The same symbol as defined in Equation (1), expressed in MVA.
- PF: The power factor, a dimensionless value applied in this planning context as **0.90**.

Equation (2) converts the source MVA rating into the MW quantity used by the neural forecast. At PF = 0.90, the two-transformer planning envelope is 113.4 MW and the one-transformer envelope is 56.7 MW. This conversion keeps the forecasting and capacity calculations in consistent units, but it must not be mistaken for a replacement for reactive-power and voltage analysis.

(3) Baseline Peak-Load Definition for 2026

$$P_{2026} = 0.80 \times P_{\text{source}} \tag{3}$$

- P_{2026}: The baseline planning peak-load value (in MW) established for the year 2026, serving as the reference starting point.
- P_{source}: The same symbol as defined in Equation (2), expressed in MW.

Equation (3) defines a transparent 2026 planning peak at 80% of the normal source capability. The value is an assumption, not a claimed SCADA maximum. Its role is to provide an auditable starting point until a validated coincident station peak is available.

(4) Ten-Year Peak-Load Projection Using Compound Growth

$$P_y = P_{2026} \times (1+g)^{(y-2026)}; y = 2027,2028,\ldots,2036 \tag{4}$$

- P_y: The forecasted peak-load value (in MW) for the target year $y$within the ten-year planning horizon.
- P_{2026}: The same symbol as defined in Equation (3), representing the base-year value for 2026.
- g: The compound annual growth rate (CAGR), expressed as a decimal (e.g., 0.05 for a 5% growth rate).
- y: The target year within the planning horizon, ranging from 2027 through 2036 inclusively.

Equation (4) extends the base peak through the ten-year horizon using a compound growth rate g. Each annual peak scales a complete 8760-hour shape; the equation does not imply that every hour grows independently or that a single growth rate will remain valid under all economic and policy conditions.

Engineering interpretation of Equations (2)-(4): these equations form a traceable chain from installed MVA to a planning MW envelope, then to a base-year loading assumption and a future capacity requirement. The chain makes the assumptions visible and shows when normal headroom is consumed. It does not prove N-1 security, because the one-transformer limit remains far below the high-load forecast for substantial parts of the year. Low, central, and high growth cases, station power factor, temperature derating, and verified feeder limits should therefore be tested together.

The preferred hourly network calculation is an AC load flow with verified positive-sequence line and transformer parameters. Because the disclosed one-line diagram does not include the complete impedance and control data, the present study uses capacity, current, voltage-deviation, and loss-duty screens. Every proxy is labelled as such, and the MATLAB configuration allows verified values to replace the assumptions without changing the HNF-ROLM decision logic.

4. NEURAL FORECASTING MODEL AND VALIDATION

The FFNN input represents time without introducing artificial discontinuities. Six Fourier terms describe the daily fundamental and its second and third harmonics, while twelve one-hot variables identify the month. This compact encoding places hour 23 close to hour 0 in feature space and allows the network to represent morning ramps, midday shoulders, evening peaks, and seasonal level changes.

The chronological split follows the source study: earlier Day-1 observations are used for training and later Day-2 observations are retained for independent testing. This is stricter than random shuffling because the model must generalize to measurements that were never intermingled with its training samples. With a small dataset, the architecture, regularization, random seed, feature definitions, and training settings must be fixed and archived.

Periodic Feature-Vector Construction

$$x_t = [\sin(2\pi h/24),\ \cos(2\pi h/24),\ \ldots,\ \sin(6\pi h/24),\ \cos(6\pi h/24),\ M_1,\ \ldots,\ M_{12}]^T \tag{5}$$

- x_t: The input feature vector presented to the neural network at time step t. It is an 18-element column vector (indicated by the transpose operator).
- h: The hour of the day, taking integer values from 0 to 23.
- $\sin(2\pi h/24),\ \cos(2\pi h/24),\ \ldots,\ \sin(6\pi h/24),\ \cos(6\pi h/24)$: Twelve elements consisting of six pairs of sine–cosine harmonic terms. These encode the cyclic nature of the 24-hour daily period, ensuring that neighboring clock times (e.g., 23:00 and 00:00) remain close to one another in the feature space.
- $M_1, \ldots, M_{12}$: Twelve binary (0/1) indicator variables representing the calendar month. For a given time step, only the variable corresponding to the current month is set to 1, while all others are set to 0. These preserve seasonal categories without imposing a false ordinal or linear relationship between months.
- $[\cdot]^T$: The transpose operator, which converts the row vector into a column vector.

Equation (5) creates an 18-element input vector. The harmonic pairs place neighbouring clock times close to one another in feature space, while the month indicators preserve seasonal categories without imposing a false linear order.

Hidden-Layer Activation

$$h_t = \tanh(W_1\, x_t + b_1) \tag{6}$$

- h_t: The hidden-layer output vector (activation values) at time step t. This vector contains **12 elements**, corresponding to the 12 neurons in the hidden layer.
- $\tanh(\cdot)$: The hyperbolic tangent activation function, applied element-wise to the vector argument. It is a bounded, differentiable, nonlinear function that outputs values in the range $(-1, +1)$.
- W_1: The input-to-hidden weight matrix. Its dimensions are 12×18, mapping the 18-element input vector to the 12 hidden neurons.
- x_t: The input feature vector defined in Equation (5).
- b_1: The bias vector for the hidden layer, containing 12 elements (one per hidden neuron).

Equation (6) calculates the twelve hidden-neuron activations. The bounded tanh function captures nonlinear interactions between hour and season while limiting activation magnitude. A larger network could fit the training set more closely, but it would not be justified without more representative data.

Conversion of Network Output to Active Power

$$\hat{P}_t = P_{\max,\text{regional}} \cdot (W_2\, h_t + b_2) \quad (7)$$

- $\hat{P}_t$: The final forecasted active power (in **MW**) at time step t. This is the denormalized network output, representing the predicted load for the specific regional station.
- $P_{\max,\text{regional}}$: The regional maximum active-power scaling factor (in MW). This is the value used to normalize the target variable during training; multiplying by it reverses the normalization, bringing the prediction back into physical MW units.
- W_2: The hidden-to-output weight vector. Its dimensions are 1×12, mapping the 12 hidden-neuron activations to a single scalar output.
- h_t: The hidden-layer activation vector defined in Equation (6).
- b_2: The output-layer bias scalar (a single numeric value).

Equation (7) reverses target normalization and expresses the prediction in MW. Negative predictions are constrained. The normalized regional shape is then transferred to the Al-Ruwais envelope.

Table 5. Neural-network configuration and reported chronological holdout performance

Item	Value
Measured observations	456 hourly values from 19 GECOL reports
Inputs	18: six Fourier terms + twelve-month indicators
Hidden layer	12 tanh neurons
Output	Normalized Western-region load
Training/test split	288 Day-1 hours / 168 later Day-2 hours
Solver in source paper	L-BFGS with L2 regularization
Reported validation MAE	115.938 MW
Reported validation RMSE	149.938 MW
Reported validation MAPE	2.944%

Table 5 preserves the performance reported in the supplied paper. When the original CSV is provided, the companion programs recompute the validation metrics from the accepted observations. Their deterministic fallback dataset is only a software-verification fixture; it must never overwrite or be confused with the measured validation record.

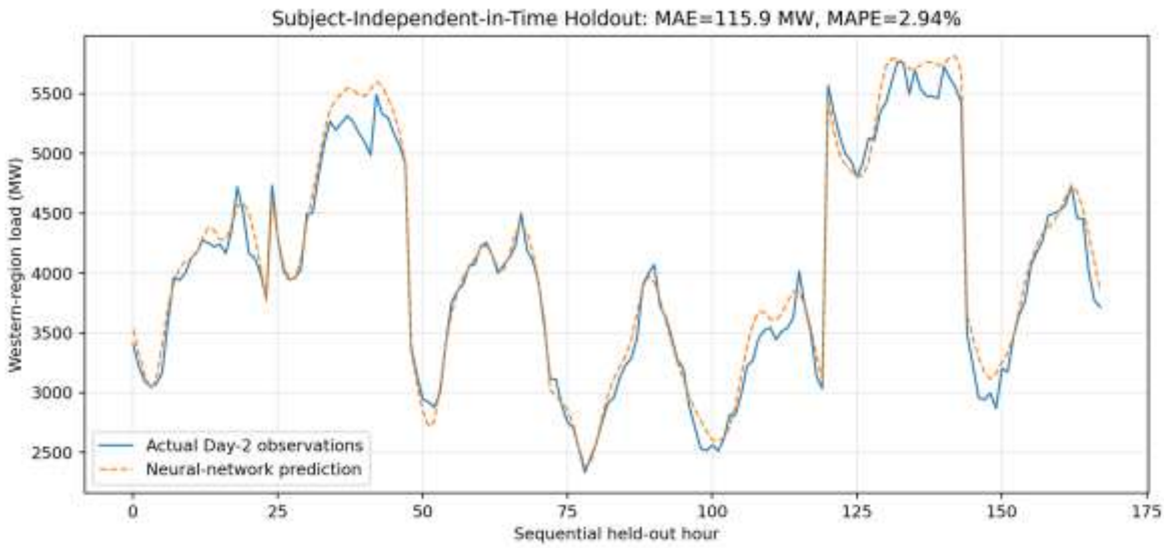

Fig. 4. Actual and predicted load on the independent chronological holdout.

The visual fit is useful, but operational attention should concentrate on underprediction during ramps and peak windows, where even a short error can exhaust the security margin.

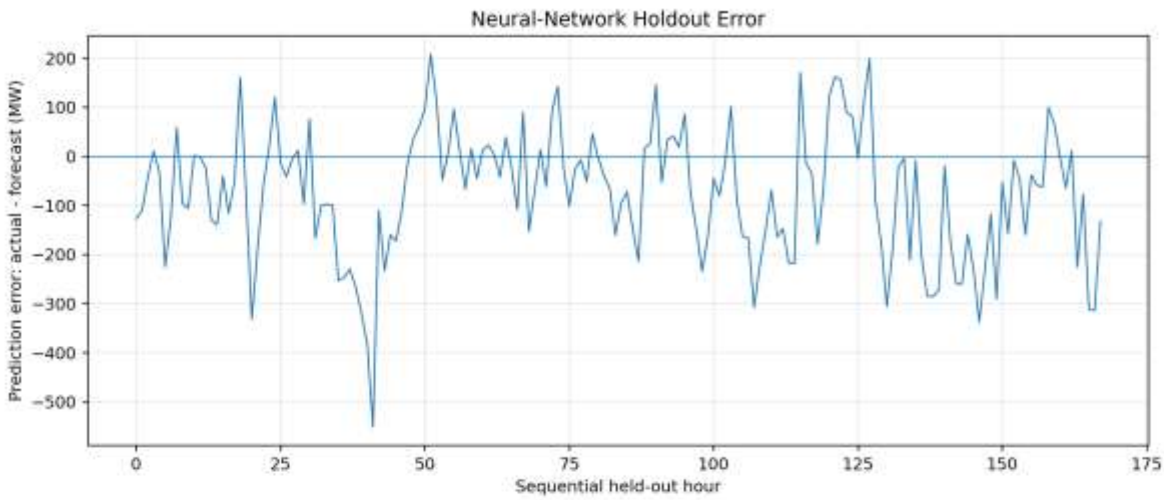

Fig. 5. Independent holdout residual, defined as actual load minus neural prediction.

A positive residual means actual load exceeded the neural estimate. Persistent positive residuals should increase the uncertainty reserve or trigger earlier corrective action.

Mean Absolute Error (MAE)

$$\mathrm{MAE} = \frac{1}{N}\sum_{t=1}^{N} \mid P_t - \hat{P}_t \mid \tag{8}$$

- MAE : The Mean Absolute Error of the forecast, expressed in the same units as the load (MW). It represents the typical magnitude of the hourly forecast error.
- N: The total number of observations (hours) in the evaluation dataset.
- P_t: The actual measured active power (in MW) at time step t.
- $\hat{P}_t$: The forecasted active power (in MW) at time step t, as produced by the neural network.
- $\sum_{t=1}^{N}$: The summation operator over all Ntime steps from $t = 1$to $t = N$.

MAE is the typical magnitude of the hourly forecast error in MW. It is easy to interpret and useful for ordinary correction and reserve discussion, but the regional MAE should not be copied directly into an Al-Ruwais reserve requirement without station-level residual analysis.

Root Mean Square Error (RMSE)

$$\mathrm{RMSE} = \sqrt{\frac{1}{N}\sum_{t=1}^{N}\left(P_t - \hat{P}_t\right)^2} \tag{9}$$

- RMSE: The Root Mean Square Error of the forecast, expressed in MW. It is a quadratic scoring metric that penalizes larger deviations more heavily than smaller ones.
- N: The total number of observations (hours) in the evaluation dataset.
- P_t: The actual measured active power (in MW) at time step t.
- $\hat{P}_t$: The forecasted active power (in MW) at time step t.
- $\sum_{t=1}^{N}$: The summation operator over all Ntime steps.
- $\sqrt{\cdot}$: The square root operator, which brings the units back to MW after summing the squared errors.

RMSE penalizes large deviations more strongly. This matters because a small number of large underforecasts near a ramp or peak can create an overload even when the average error appears modest.

Mean Absolute Percentage Error (MAPE)

$$\mathrm{MAPE} = \frac{100}{N}\sum_{t=1}^{N} \left| \frac{P_t - \hat{P}_t}{P_t} \right| \tag{10}$$

- MAPE : The Mean Absolute Percentage Error, expressed as a percentage (%). It measures forecast accuracy relative to the magnitude of the actual load.
- N: The total number of observations (hours) in the evaluation dataset.
- P_t: The actual measured active power (in MW) at time step t. This value must be **non-zero** for the fraction to be defined.
- $\hat{P}_t$: The forecasted active power (in MW) at time step t.
- $\sum_{t=1}^{N}$: The summation operator over all Ntime steps.

MAPE expresses error relative to the actual load and supports comparison between the regional scale and a smaller station envelope. It should be used only when actual load is nonzero and should be read with residual plots, bias, peak-window error, and uncertainty bands.

Engineering interpretation of Equations (5)-(10): Equations (5)-(7) turn calendar structure into a physical MW prediction; Equations (8)-(10) test the quality of that prediction. HNF-ROLM adds the operational question that the statistical metrics cannot answer: after the forecast is compared with network limits, does the selected action preserve service and reduce the consequences of the disturbance?

Table 6. Meaning and engineering use of the forecasting and resilience indicators

Indicator	What it measures	How it is used in this study
MAE	Typical absolute forecasting error in MW	Ordinary correction and forecast-quality interpretation
RMSE	Forecast error with extra weight on large deviations	Sensitivity to peak and ramp errors
MAPE	Average relative forecasting error	Comparison across load scales
ENS	Electrical energy not served after all corrective actions	Direct measure of lost service
SAIDI	Average interruption duration	Load-weighted planning proxy until customer records are available
SAIFI	Average interruption frequency	Load-weighted planning proxy until event records are available
RI	Composite index from 0 to 1; higher is better	Ranks decisions using ENS, SAIDI, SAIFI, and violation hours

5. CONSTRUCTION OF THE TEN-YEAR HOURLY FORECAST

After model selection, the FFNN is fitted to all accepted observations. A representative 24-hour curve is generated for each month, neighbouring monthly behaviour is blended through the calendar, and the first annual series is calibrated to the disclosed peaks and energies. The 2028-2036 series are then obtained by applying the compound annual growth multiplier to the complete chronology. In this way, the daily and seasonal shape comes from the measured regional evidence, while the absolute Al-Ruwais level comes from the stated asset and growth assumptions.

A standardized non-leap year is retained in each planning case so that energy, peak, and reliability indicators can be compared without a calendar-length effect. This is a modelling convention, not a claim that leap-day demand is irrelevant. A live operational version should use the real calendar and update the forecast with SCADA, weather, outage, tariff, holiday, and distributed-generation information.

Annual Energy Calculation by Hourly Integration

$$E_y = \frac{\Delta t}{1000} \sum_{t=1}^{8760} P_{(y,t)} \tag{11}$$

- E_y: The total annual electrical energy for year y, expressed in **GWh** (gigawatt-hours).
- Δt: The time-step interval between successive samples, expressed in **hours**. For an hourly time series, $\Delta t = 1$hour.
- 1000: The conversion factor used to convert from **MWh** to **GWh**, since 1 GWh $=$ 1000 MWh.
- $\sum_{t=1}^{8760}$: The summation operator over all hours of a standard year, from hour $t = 1$to hour $t = 8760$.
- $P_{(y,t)}$: The active power (in **MW**) recorded or forecasted for year $y$at hour t.

Equation (11) integrates the hourly series. With a one-hour step, MW multiplied by hours gives MWh, and division by 1000 gives GWh. Annual energy governs PV contribution, storage cycling, purchase planning, and ENS normalization; it cannot be inferred reliably from the annual peak.

Annual Load-Factor Calculation

$$\mathrm{LF}_y = \frac{1000 \times E_y}{8760 \times P_{\mathrm{peak},y}} \tag{12}$$

- LF_y: The annual load factor for year y. This is a dimensionless ratio (often expressed as a decimal or percentage) that indicates the average utilization of the peak demand over the year.
- 1000: The conversion factor that reconciles the units. Since $E_y$is in **GWh** and $P_{\mathrm{peak},y} \times 8760$yields **MWh**, multiplying by 1000 converts the numerator to MWh, making the ratio consistent. (Alternatively, it keeps the denominator in GWh when dividing by 1000).
- E_y: The total annual energy for year y, as defined in Equation (11), expressed in **GWh**.
- 8760: The total number of hours in a standard (non-leap) year.
- $P_{\mathrm{peak},y}$: The annual peak active power (in **MW**) recorded or forecasted for year y.

Equation (12) compares annual energy with the energy that would be used if the annual peak persisted continuously. The load factor distinguishes peak capability from sustained energy duty and is especially useful when deciding whether storage requires a high MW rating, a long MWh duration, or both.

Engineering interpretation of Equations (11)-(12): the peak determines transfer capability, while integrated energy determines sustained resource duty. A moderate load factor can coexist with a serious short-duration overload, which is why the complete chronology is retained instead of replacing the year with a single peak and average.

5.1 Ten-Year Capacity and Energy Results

Table 7. Ten-year neural forecast and RI-triggered adaptive capacity screen

Year	Peak MW	Energy GWh	Normal MW	N-1 MW	Model action
2027	97.978	575.295	113.4	56.7	Operate existing assets
2028	105.816	621.319	113.4	56.7	Operate existing assets
2029	114.282	671.024	113.4	56.7	Trigger reinforcement for 2030
2030	123.424	724.706	170.1	113.4	Commission equivalent 63-MVA transfer block
2031	133.298	782.682	170.1	113.4	Operate existing assets
2032	143.962	845.297	170.1	113.4	Operate existing assets
2033	155.479	912.921	170.1	113.4	Operate existing assets
2034	167.917	985.955	170.1	113.4	Trigger reinforcement for 2035
2035	181.350	1064.831	226.8	170.1	Commission equivalent 63-MVA transfer block
2036	195.858	1150.017	226.8	170.1	Operate existing assets

The actions in Table 7 are model signals, not construction commitments. They identify the years by which technically equivalent transfer capability should be in service if the central growth assumption, the present flexibility portfolio, and the RI threshold remain valid. A formal investment decision must also consider construction lead time, outage windows, lifecycle cost, land, protection, permitting, and alternative transfer paths.

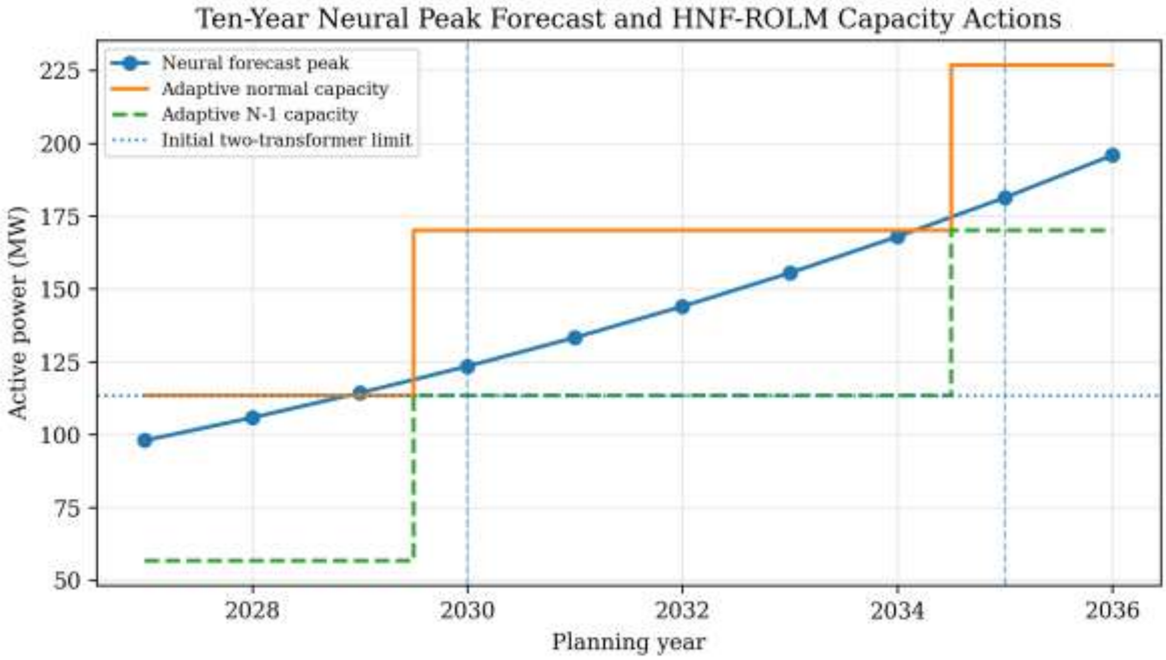

Fig. 6. Ten-year neural peak forecast, adaptive normal capacity, and N-1 capacity actions.

Reinforcement must be available before firm capacity is crossed. Under the central assumptions, the model signals commissioning in 2030 and again in 2035.

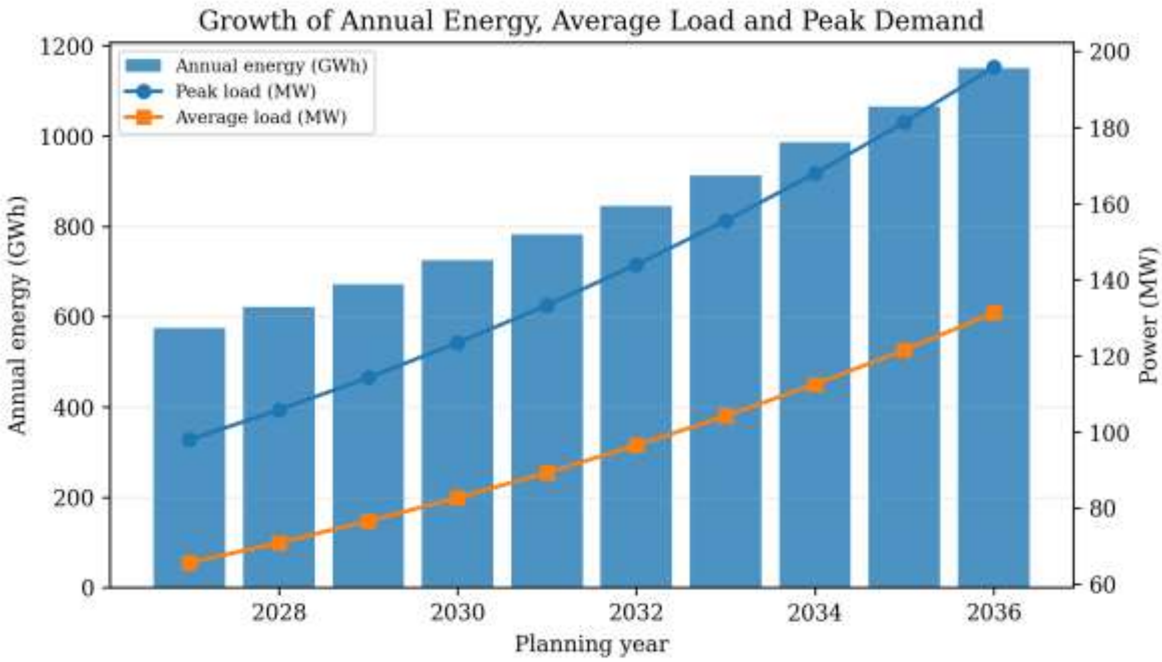

Fig. 7. Growth of annual energy, average demand, and peak demand over the planning horizon.

Peak demand determines transfer capability, whereas annual energy determines sustained resource duty. Storage therefore requires coordinated MW and MWh sizing.

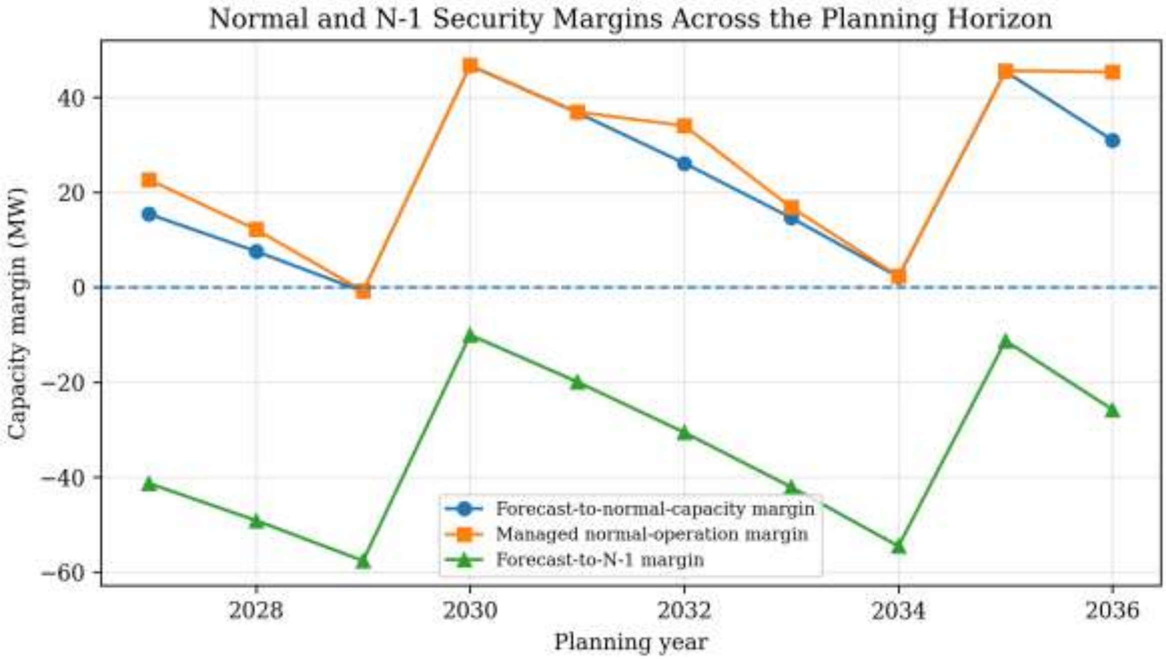

Fig. 8. Normal and N-1 security margins before and after the HNF-ROLM capacity actions.

A positive normal margin can coexist with a negative N-1 margin. Normal adequacy must never be reported as contingency adequacy.

The normal-capacity margin narrows quickly before each reinforcement step. In contrast, the N-1 margin remains negative for many high-load hours even after operational coordination. This distinction is crucial: spare headroom with all equipment in service is not the same as resilience during a transformer outage. HNF-ROLM therefore treats reinforcement timing and short-duration flexibility as complementary decisions, not interchangeable substitutes.

5.2 Resource and Resilience Comparisons

Table 8. Ten-year resilience indicators before and after HNF-ROLM coordination

Year	ENS MWh Base / HNF	SAIDI h Base / HNF	SAIFI Base / HNF	RI Base / HNF
2027	262.5 / 126.6	2.748 / 1.339	0.421 / 0.345	0.895 / 0.939
2028	315.9 / 197.6	3.063 / 1.926	0.464 / 0.416	0.884 / 0.919
2029	402.1 / 377.8	3.635 / 3.391	0.615 / 0.536	0.845 / 0.860
2030	39.2 / 0.0	0.321 / 0.000	0.081 / 0.000	0.982 / 1.000
2031	106.4 / 6.4	0.815 / 0.049	0.149 / 0.037	0.964 / 0.995
2032	179.1 / 58.7	1.273 / 0.428	0.212 / 0.177	0.948 / 0.976
2033	257.6 / 135.1	1.697 / 0.900	0.271 / 0.261	0.932 / 0.957
2034	364.6 / 342.4	2.242 / 2.090	0.379 / 0.325	0.908 / 0.918
2035	40.7 / 0.0	0.227 / 0.000	0.062 / 0.000	0.986 / 1.000
2036	136.0 / 30.7	0.708 / 0.165	0.132 / 0.069	0.968 / 0.990

Table 9. Incremental 2027 comparison of conventional operation and flexible-resource scenarios

Scenario	Peak MW	ENS MWh	SAIDI h	SAIFI	RI
Conventional	97.978	271.1	2.837	0.421	0.892
PV only	97.978	262.5	2.748	0.421	0.895
PV+BESS	97.880	186.6	1.964	0.414	0.918

Scenario	Peak MW	ENS MWh	SAIDI h	SAIFI	RI
PV+BESS+DR	89.831	126.6	1.339	0.345	0.939

Table 9 separates the contribution of each flexible resource. PV lowers annual energy import and daytime loading, but it does not materially reduce the evening monthly peak in this load shape. BESS provides firm time shifting and removes much of the short-duration peak. DR becomes most valuable when the battery reaches a power, energy, or SOC constraint, and it further reduces the unserved part of the N-1 event. The incremental comparison makes clear why the resources should be coordinated rather than sized independently.

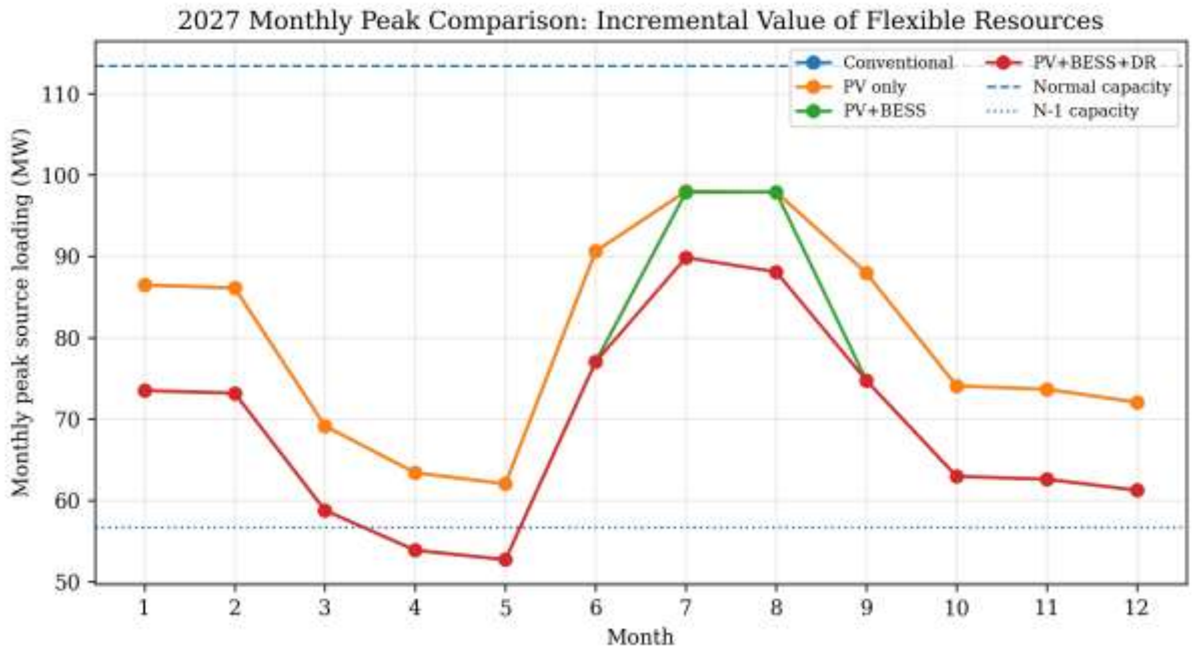

Fig. 9. Monthly 2027 source-loading comparison for conventional, PV-only, PV+BESS, and PV+BESS+DR operation.

PV reduces daytime import, while BESS and DR address the evening peak. The timing of each resource is more important than its annual energy contribution alone.

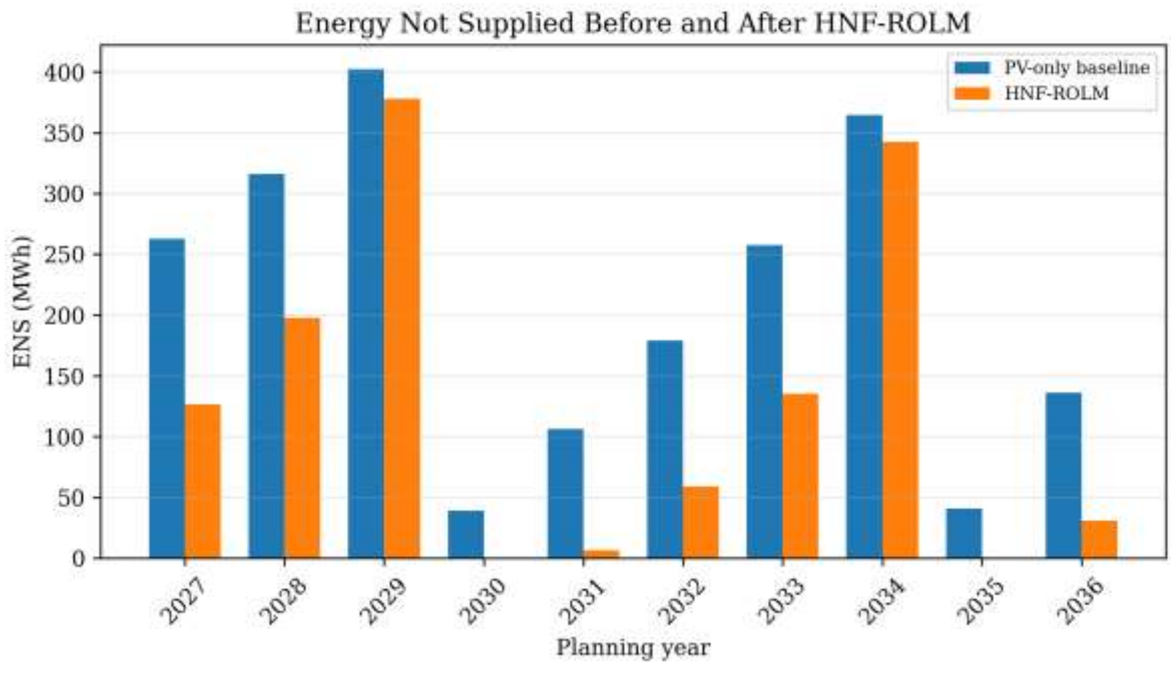

Fig. 10. Energy Not Supplied before and after HNF-ROLM across the ten-year horizon.

Lower ENS means more customer energy is preserved. Any remaining ENS identifies hours that require firmer capacity, additional flexibility, or revised load priorities.

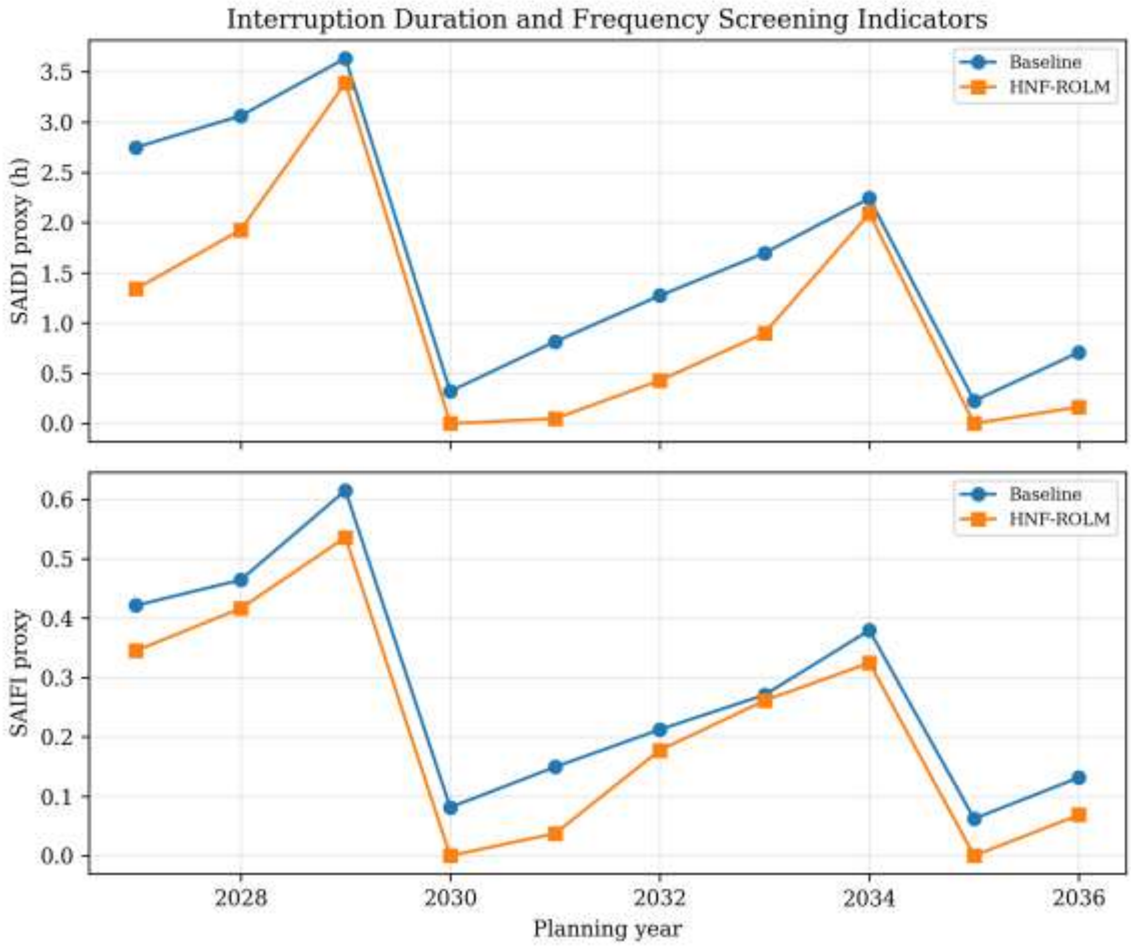

Fig. 11. Load-weighted SAIDI and SAIFI screening indicators before and after coordination.

The plotted SAIDI and SAIFI values are load-weighted planning proxies. Official utility indices require verified customer counts, interruption zones, and restoration records.

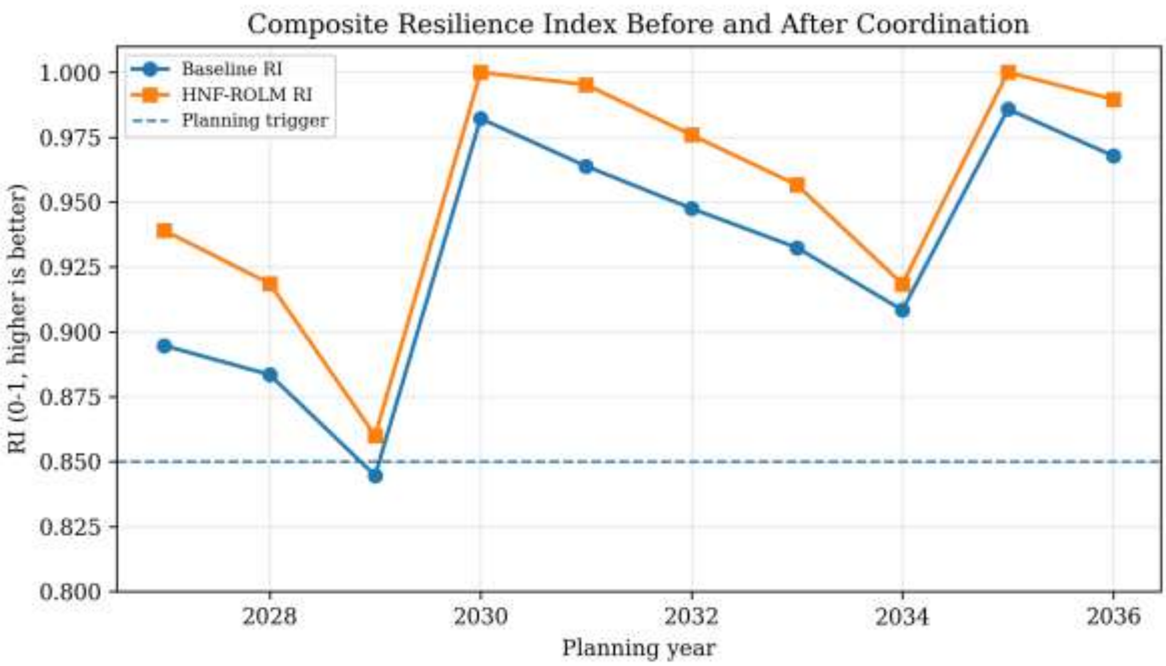

Fig. 12. Composite Resilience Index before and after coordination, including the planning trigger.

The RI threshold is a transparent planning rule, not a universal standard. Its weights should be calibrated to GECOL policy and critical-load priorities.

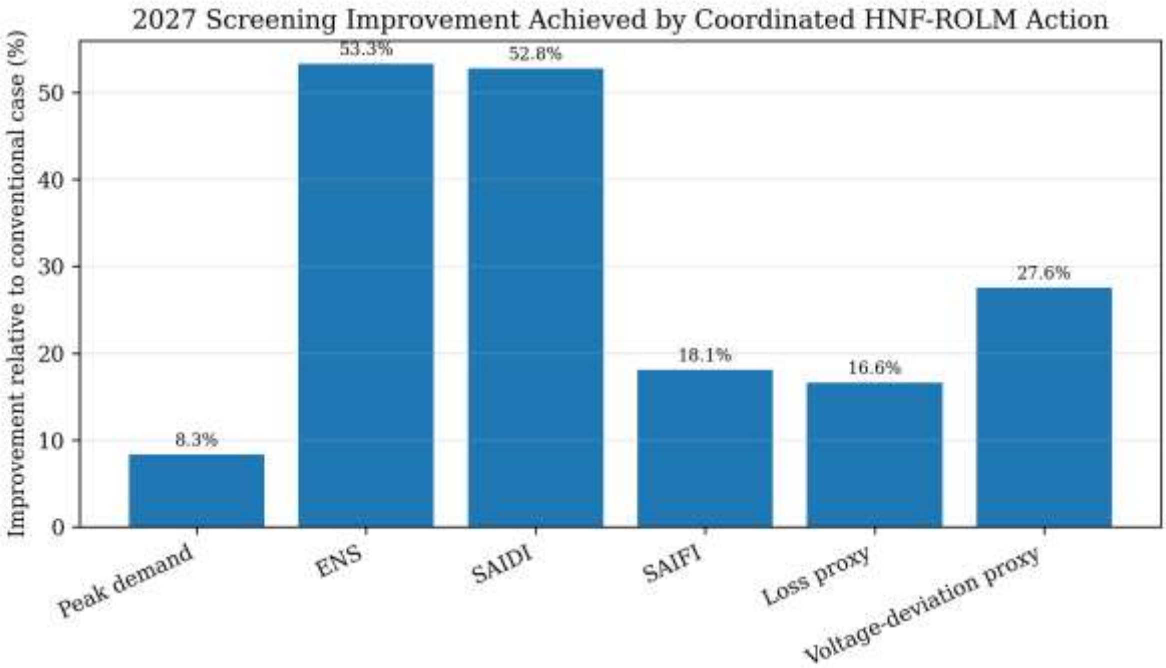

Fig. 13. First-year improvement in peak, service, and screening indicators under coordinated action.

No single KPI is sufficient. Peak reduction, ENS, SAIDI, SAIFI, and RI must be read together before an operating strategy is accepted.

In the first planning year, coordinated operation reduces the screened peak by about eight percent, cuts ENS and SAIDI by approximately one half, lowers SAIFI, and increases RI from roughly 0.89 to 0.94. The gain is substantial but not unlimited. The 2029 case approaches the original capacity limit, and the second reinforcement signal appears by 2034 for commissioning in 2035. The result is physically intuitive: flexibility manages short peaks and disturbances, whereas persistent demand growth eventually requires additional firm transfer capability.

6. PROBLEM REFORMULATION

The forecasting task is reformulated as a constrained chronological coordination problem. Forecast demand and available PV are external time-series inputs. BESS power, DR reduction, PV curtailment, verified feeder transfer, reinforcement status, and involuntary shedding are decisions. Source loading, bus voltage, feeder current, losses, and BESS state of charge are calculated states. This separation prevents the neural network from being mistaken for the control policy.

Managed Net-Load Balance

$$P_{\mathrm{net},t} = \hat{P}_t - P_{\mathrm{PV},t} + P_{\mathrm{ch},t} - P_{\mathrm{dis},t} - P_{\mathrm{DR},t} - P_{\mathrm{LS},t} \qquad (13)$$

- $P_{\mathrm{net},t}$: The net active power (in MW) that must be supplied by the source transformers at time step t.
- $\hat{P}_t$: The forecasted active-power load (in MW) at time step t, as produced by the neural network.
- $P_{\mathrm{PV},t}$: The active-power output (in MW) from photovoltaic (PV) generation at time step t. This term reduces the source duty.
- $P_{\mathrm{ch},t}$: The active power (in MW) consumed by battery energy storage system (BESS) charging at time step t. This term increases the source duty.

- $P_{\mathrm{dis},t}$: The active power (in MW) supplied by BESS discharging at time step t. This term reduces the source duty.
- $P_{\mathrm{DR},t}$: The active-power reduction (in MW) achieved through demand response (DR) programs at time step t. This term reduces the net load.
- $P_{\mathrm{LS},t}$: The active power (in MW) that is deliberately shed or left unsupplied as a last-resort measure at time step t. This term also reduces the net load requirement.

Equation (13) is the bridge between prediction and operation. PV and battery discharge reduce source duty; battery charging increases it; DR changes scheduled consumption; and P_LS,t represents last-resort unsupplied load. Once the forecast enters this balance, it is no longer an isolated number—it becomes an input to a physical operating decision.

Effective Transformer-Feeder Limit

$$C_t = \min\left\{P_{T,t}^{\max},\ P_{\mathrm{line},t}^{\max}\right\} \tag{14}$$

- C_t: The most restrictive verified active-power transfer limit (in MW) applicable at time step t. This is the maximum permissible load that can be served.
- $P_{T,t}^{\max}$: The maximum active-power capacity (in MW) of the source transformer bank at time step t.
- $P_{\mathrm{line},t}^{\max}$: The maximum active-power capacity (in MW) of the feeder lines at time step t.
- $\min\{\cdot\}$: The minimum operator, which selects the smaller value between the two limits.

Equation (14) applies the most restrictive verified transfer limit. In the present screen, the transformer envelope governs because final conductor ampacities are not disclosed. Both programs expose a feeder-limit parameter so that verified values can be inserted directly without changing the decision logic.

Energy Not Supplied

$$\mathrm{ENS}_y = \sum_t P_{\mathrm{LS},t}\ \Delta t \tag{15}$$

- ENS_y: The total Energy Not Supplied (in **MWh**) during year y.
- $P_{\mathrm{LS},t}$: The active power (in MW) that is shed or left unsupplied at time step t, as defined in Equation (13).
- Δt: The time-step interval (in hours) between successive samples.
- $\sum_t$: The summation operator over all time steps within the study period (e.g., across all hours of the year).

ENS is the total electrical energy that cannot be served after lower-cost flexibility has been exhausted. It converts an overload from an abstract constraint violation into a direct service consequence and is therefore the most heavily weighted term in the present RI.

System Average Interruption Duration Index (SAIDI)

$$\mathrm{SAIDI}_y = \frac{\sum_i N_i\ U_i}{\sum_i N_i} \tag{16}$$

- SAIDI_y: The System Average Interruption Duration Index for year y, expressed in **minutes per customer** (or hours per customer, depending on the unit of U_i). It represents the average duration of interruptions experienced by a served customer.
- N_i: The number of customers connected to load zone or feeder i.
- U_i: The average interruption duration (in minutes or hours) experienced by customers in zone $i$over the year.
- $\sum_i$: The summation operator over all load zones or feeders.

System Average Interruption Frequency Index (SAIFI)

$$\text{SAIFI}_y = \frac{\sum_i N_i \ \lambda_i}{\sum_i N_i} \tag{17}$$

- SAIFI_y: The System Average Interruption Frequency Index for year y, expressed in **interruptions per customer**. It represents the average number of interruptions experienced by a served customer.
- N_i: The number of customers connected to load zone or feeder i.
- λ_i: The average interruption frequency (number of interruptions per customer) experienced in zone $i$over the year.
- $\sum_i$: The summation operator over all load zones or feeders.

Equations (16) and (17) are the conventional customer-weighted forms. Because verified customer counts, interruption zones, relay operations, and restoration records are unavailable, this numerical study reports transparent load-weighted planning proxies. They are suitable for comparing scenarios but must not be presented as official regulatory indices.

Composite Resilience Index

$$\text{RI}_y = 1 - [0.45\ \bar{\text{ENS}}_y + 0.25\ \bar{\text{SAIDI}}_y + 0.15\ \bar{\text{SAIFI}}_y + 0.15\ \bar{H}_{\text{viol},y}] \tag{18}$$

- RI_y: The Composite Resilience Index for year y. This is a dimensionless value between **0** and **1**, where a higher value indicates that more service is preserved and the system is more resilient.
- $\bar{\text{ENS}}_y$: The normalized value of Energy Not Supplied for year y(scaled to a common reference range, typically between 0 and 1).
- $\bar{\text{SAIDI}}_y$: The normalized value of the System Average Interruption Duration Index for year y.
- $\bar{\text{SAIFI}}_y$: The normalized value of the System Average Interruption Frequency Index for year y.
- $\bar{H}_{\text{viol},y}$: The normalized value of the total hours (or count) of constraint violations (e.g., overloads, voltage deviations) recorded during year y.
- 0.45: The weighting factor assigned to ENS (45% weight).
- 0.25: The weighting factor assigned to SAIDI (25% weight).
- 0.15: The weighting factor assigned to SAIFI (15% weight).
- 0.15: The weighting factor assigned to violation hours (15% weight).
- $1 - [\cdot]$: The subtraction from unity ensures that lower normalized penalties yield a higher resilience index.

Equation (18) combines normalized unserved energy, interruption duration, interruption frequency, and violation hours into a value between zero and one. A higher RI means that more service is preserved. The weights are visible planning assumptions; GECOL can recalibrate them to reflect utility policy, critical-load priorities, social consequences, or regulatory criteria.

The complete objective also includes capacity violation, voltage deviation, active-power loss, PV curtailment, BESS throughput and degradation, DR inconvenience, controlled shedding, and reinforcement cost. Constraints cover active and reactive power balance; transformer MVA and feeder-current limits; voltage criteria; PV and inverter capability; BESS power, efficiency, energy, and terminal SOC; DR magnitude, duration, rebound, and availability; nonnegative bounded shedding; and normal or N-1 topology. [17]

Forecast and PV uncertainty may be represented by deterministic bands, representative scenarios, or robust and chance-constrained formulations. Equipment outages are introduced by changing topology and available ratings. The same service-based formulation can therefore compare normal operation, positive forecast error, rapid PV reduction, feeder derating, transformer outage, official-holiday behaviour, seasonal stress, and blackout restoration.

Engineering interpretation of Equations (13)-(18): HNF-ROLM converts the forecast into managed net load, compares that load with physical limits, quantifies any service that remains unserved, and ranks the resulting decision through RI. Forecast accuracy remains necessary, but the preferred action is the one that stays feasible and preserves the greatest practical level of service under the declared disturbance.

7. HNF-ROLM SOLUTION ALGORITHM

HNF-ROLM means Hybrid Neural Forecasting–Resilience-Oriented Load Management. It is hybrid because the FFNN forecasting layer is coupled to a constraint-based operating and planning layer. It is resilience-oriented because every action is evaluated through ENS, SAIDI, SAIFI, RI, and violation hours rather than forecast error alone. The algorithm answers two questions in sequence: what load is expected, and which feasible combination of resources preserves the most service when that load is compared with transformer and feeder limits?

The operating sequence is deliberately practical. Available PV serves local demand first. The BESS charges during lower-risk periods and discharges as the security margin deteriorates. DR is then activated within its power, duration, and rebound limits. Verified transfer or network reconfiguration is considered next. Controlled shedding is applied only if the system remains infeasible. In parallel, a planning trigger is issued when the forecast repeatedly approaches the normal limit or when RI falls below its threshold.

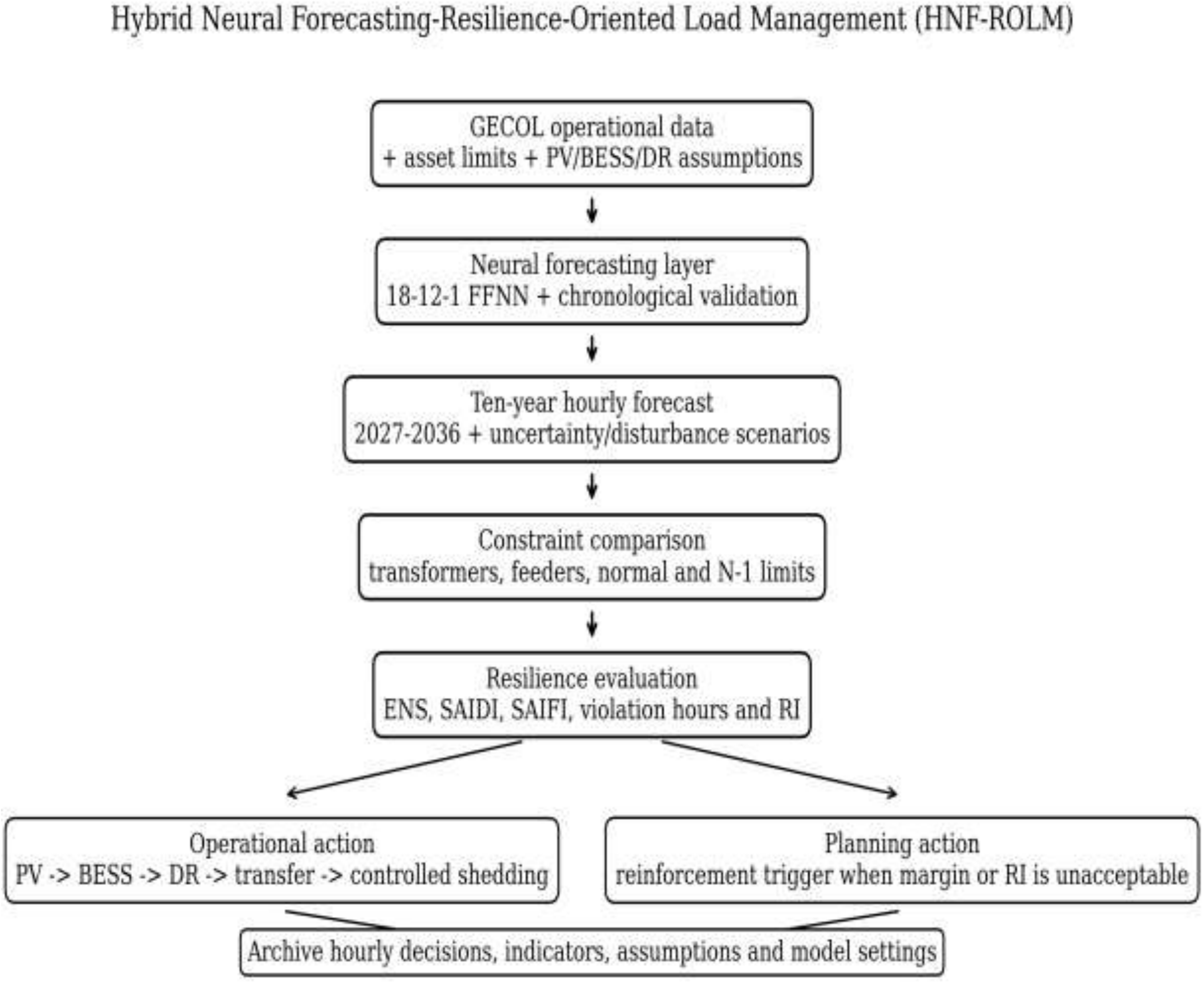

Fig. 14. Proposed HNF-ROLM architecture linking neural forecasting, operational action, resilience indicators, and reinforcement timing.

The forecast is only the first stage. The constraint and resilience layers are what convert the predicted MW value into an auditable operating or investment decision.

Table 10. Reproducible solution algorithm for the Al-Ruwais ten-year study

Step	Operation	Implementation detail
1	Data acquisition	Import GECOL measurements, asset data, PV/BESS/DR assumptions, and preserve timestamps.
2	Data validation	Check units, duplicate hours, missing values, generation-demand balance, frequency, and shedding fields.
3	Feature construction	Generate six Fourier terms and twelve-month indicators; normalize the target.
4	Chronological holdout	Train on earlier observations and test on later observations; compute MAE, RMSE, MAPE, bias, and residual curves.
5	Final FFNN fit	Refit the selected 18-12-1 network to all accepted observations using archived settings.
6	Annual assembly	Build the 8760-hour 2027 curve, calibrate monthly peaks and energy, and extend it to 2036.
7	Resource profiles	Create PV availability, BESS limits and SOC, DR windows, transfer options, and shedding priorities.
8	Forecast-to-limit comparison	Compare each predicted hour with transformer and verified feeder limits in normal and N-1 states.
9	Coordinated dispatch	Apply PV, BESS, DR, transfer, and controlled shedding in the declared order.
10	Network screen	Calculate source loading, current, voltage/loss proxies or AC load flow, and constraint violations.
11	Resilience evaluation	Compute ENS, SAIDI, SAIFI, violation hours, and RI before and after control.
12	Disturbance loop	Repeat for load error, PV reduction, feeder derating, transformer outage, and reduced flexibility availability.
13	Planning trigger	Schedule equivalent transfer reinforcement when margin or RI is unacceptable after corrective action.
14	Verification and reporting	Check energy balance, SOC continuity, solver status, infeasible hours, and export auditable tables and figures.

7.1 From Forecast to an Operating Decision

At the beginning of every operating interval, the latest timestamp, weather and calendar flags, equipment availability, and measured load are validated. The FNN produces the next-hour demand estimate, and a risk-adjusted value is formed by adding an uncertainty allowance derived from recent residuals. Available PV is then subtracted to obtain the unmanaged source requirement.

That requirement is compared with the effective transformer-feeder limit. When the margin is comfortable, the algorithm may charge the battery while preserving an SOC reserve. As the margin narrows, charging stops, BESS discharge begins, and DR is called within its contractual limits. Verified transfer or reconfiguration follows. Controlled shedding is used only for the remaining infeasible portion. The selected action is accepted only after energy balance, SOC continuity, equipment limits, and resilience indicators have been checked.

Table 11. Forecast-to-decision operating rules and safeguards

Risk-adjusted loading condition	Primary decision	Mandatory safeguard
Net load ≤ 0.62 C_t	Serve load and charge BESS when headroom and SOC permit.	Do not reduce contingency reserve or violate terminal SOC.
0.62 C_t < net load ≤ 0.85 C_t	Operate normally; stop unnecessary charging and preserve flexibility.	Monitor residual bias, PV ramp risk, and outage state.
0.85 C_t < net load ≤ C_t	Discharge BESS, then activate DR as the margin declines.	Respect BESS MW/MWh, SOC, DR duration, rebound, and availability.
Net load > C_t	Use BESS + DR + verified transfer/reconfiguration; shed only the residual gap.	Protect critical loads, log ENS, and report the infeasible hour.
Contingency or blackout	Replace C_t with the available island/contingency capability and restore by priority.	Grid-forming source, protection, communications, and black-start sequence must be verified.

7.2 Behavior After One Hour, One Year, Ten Years, and Special Conditions

After one hour. The loop is closed with the newest measurement. Forecast error is calculated, the residual history and SOC are updated, and the action for the following hour is recomputed. A large positive residual or an unexpected PV drop raises the reserve requirement immediately; the algorithm does not wait for annual retraining.

After one year. The full year is reviewed for MAE, RMSE, MAPE, bias, peak-window error, ENS, SAIDI, SAIFI, RI, violation hours, battery throughput, DR use, rebound, and unserved critical load. The model is then retrained or recalibrated with the accepted year of SCADA, weather, outage, and calendar data, while degraded BESS capacity and changing customer behaviour are carried into the next planning year.

After ten years. The annual forecast, flexibility portfolio, and RI trigger are evaluated sequentially from 2027 to 2036. Under the central 8% growth assumption and the stated resource sizes, the present study signals an equivalent 63-MVA transfer block for 2030 and another for 2035. These are planning dates that must be advanced by the required engineering, procurement, and outage lead time.

During official holidays. A holiday flag modifies the expected load shape and the availability of voluntary DR. Fixed-date holidays can be entered directly; religious and lunar-calendar holidays must be updated for each real year. Critical public services are protected, and the controller avoids relying on DR customers who are not contractually available during the holiday.

During spring. Lower cooling demand and stronger midday PV usually create charging opportunities. The controller stores surplus headroom for the evening ramp and retains reserve for rapid cloud, dust, or feeder events rather than curtailing PV prematurely.

During summer. Cooling demand, conductor and transformer temperature, PV module derating, and dust or soiling are treated as concurrent stressors. The BESS is pre-charged before the evening peak, DR readiness is checked, and N-1 headroom is monitored more conservatively than in mild seasons.

During a blackout. Upstream capacity is set to zero. Service can continue only in a deliberately designed island with a verified grid-forming BESS or another black-start source, compatible protection, communications, and a restoration sequence. Critical loads are energized first, PV is reconnected only after a stable voltage and frequency reference exists, and lower-priority load is added in blocks. Without these facilities, the model records unserved energy and waits for upstream restoration; ordinary grid-following PV cannot energize a dead bus by itself.

7.3 Implementation, Reproducibility, and Audit Trail

The MATLAB and Python versions use the same configuration values, feature vector, chronological split, growth model, dispatch order, disturbance definitions, and output schema. Both create machine-readable tables for validation, one-hour decisions, seasonal and holiday scenarios, blackout response, ten-year indicators, and reinforcement signals. Agreement is expected at the engineering-decision level; small numerical differences can arise from random initialization and floating-point implementations and must be documented rather than hidden.

The algorithm is designed to fail transparently. Missing data, duplicate timestamps, nonconvergent load flow, an infeasible hour, terminal-SOC mismatch, or any solver status other than optimal must be reported rather than silently repaired. This audit trail is particularly important when an output is used to justify an operating limit, a switching instruction, or an investment date.

The mandatory MATLAB file is a self-contained base-MATLAB function. It trains the 18-12-1 FFNN with an internal Adam routine, constructs the ten-year series, evaluates incremental operating strategies, applies disturbance and calendar scenarios, calculates all indicators, produces figures, and exports CSV and MAT results. The companion Python program independently mirrors the same workflow with NumPy, pandas, and Matplotlib [18].

8. DISTURBANCE AND SYSTEM RESPONSE CURVES

A disturbance is any change that moves the network away from its forecast operating point. The scenarios examined here include positive load-forecast error, rapid PV reduction, temporary source or feeder derating, a transformer N-1 outage, reduced storage or DR availability, seasonal operating conditions, official holidays, and blackout restoration. Response variables include source loading, available capacity, PV output, BESS power and SOC, DR activation, controlled shedding, and the resulting service indicators.

Figure 15 illustrates a representative high-load summer day. PV reduces daytime source duty, the BESS shifts energy into the evening period, and DR provides an additional response when storage alone cannot maintain the target. The figure also shows why a battery must be specified in both MW and MWh: a high-power rating is useful only while enough stored energy remains.

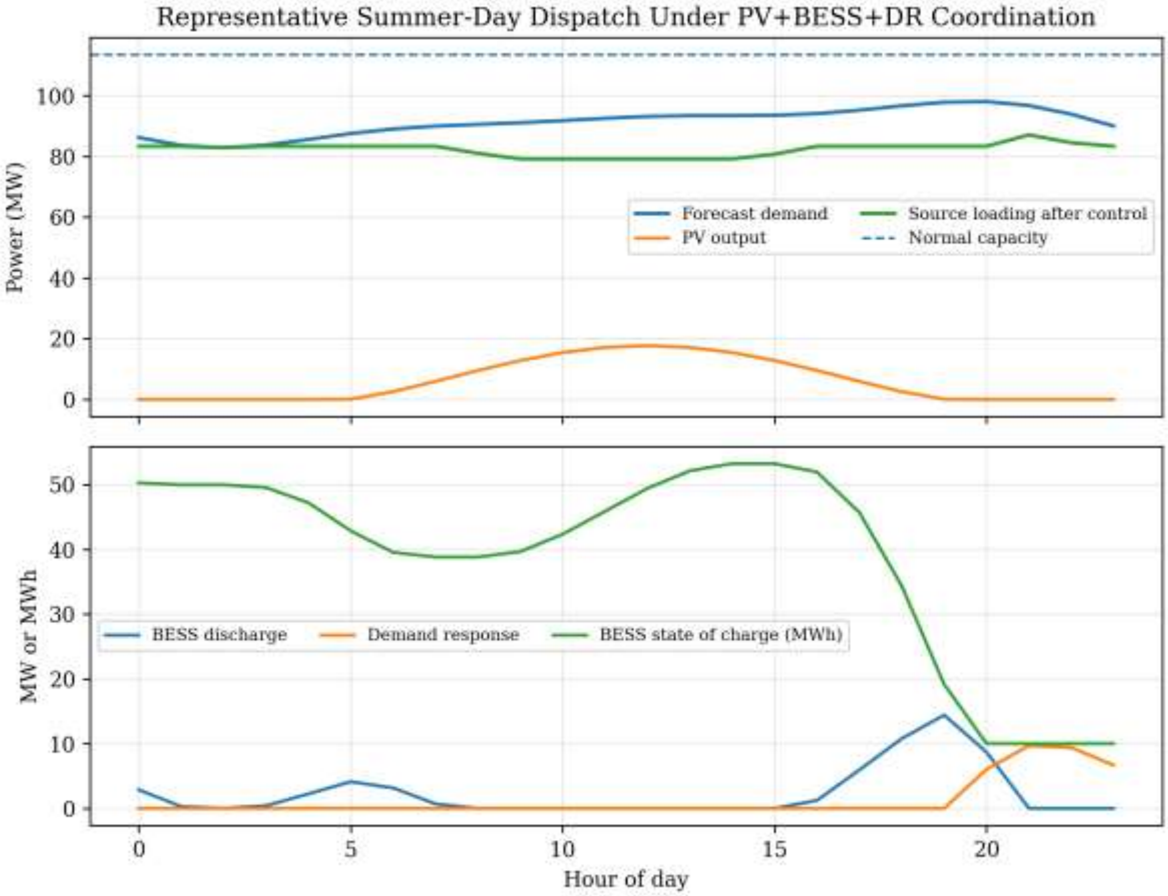

Fig. 15. Representative summer-day dispatch showing demand, PV, source loading, BESS action, DR, and state of charge.

Summer control should pre-charge the BESS before the evening ramp and account for temperature, dust, and soiling derating of PV and electrical equipment.

The transformer N-1 event in Figure 16 is more severe. Available capacity falls abruptly while forecast demand remains high. HNF-ROLM discharges the battery and activates DR before applying controlled shedding. Source loading is held at the available limit, but the remaining gap demonstrates that the initial network cannot claim N-1 adequacy from flexible resources alone. This physical shortfall is the reason for the reinforcement trigger.

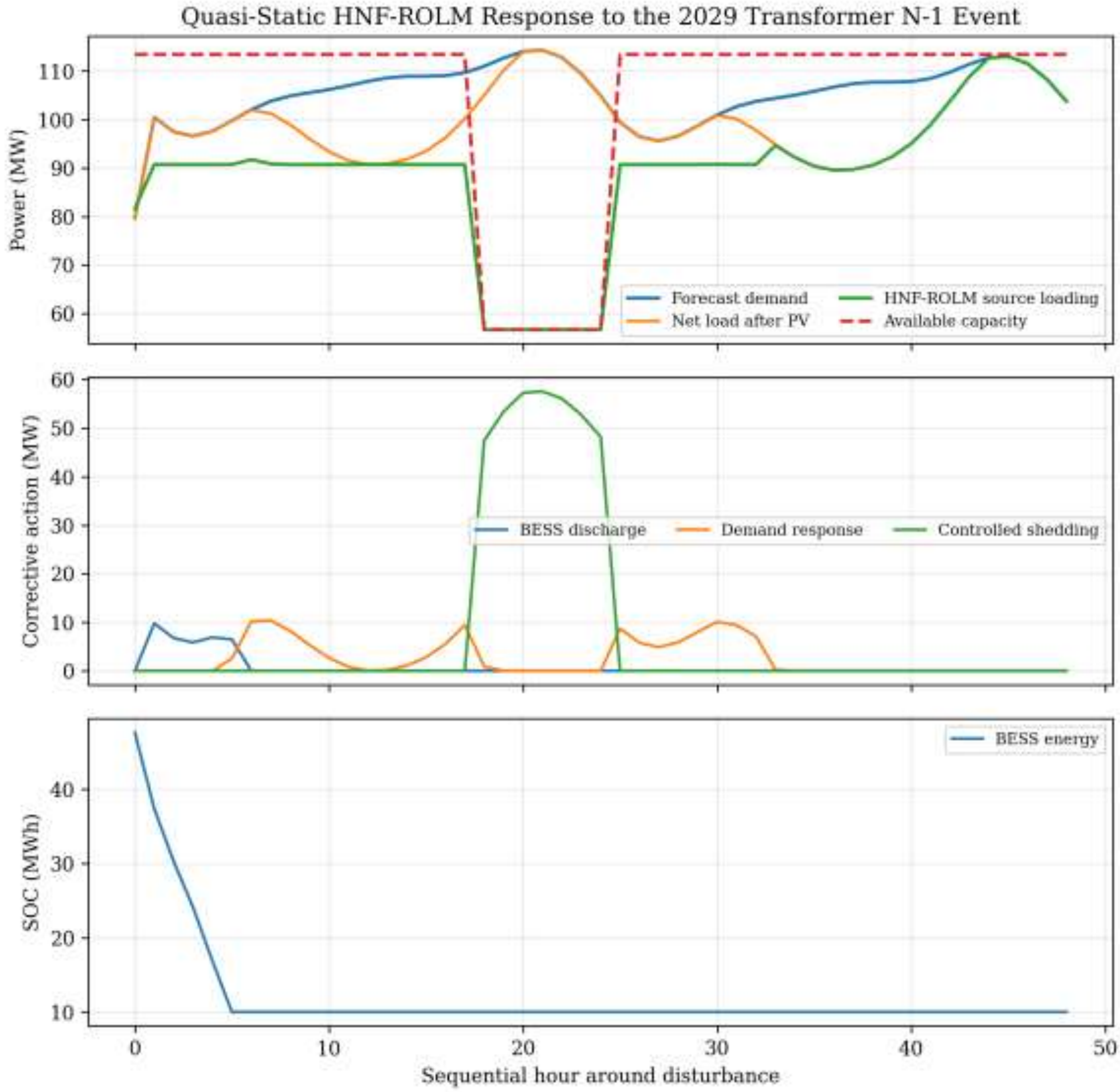

Fig. 16. Quasi-static HNF-ROLM response to the representative 2029 transformer N-1 event.

During N-1 operation, BESS and DR are deployed before controlled shedding. The remaining gap confirms that flexible resources alone cannot establish full initial N-1 adequacy.

Figure 17 adds two screening proxies. The voltage curve is a transparent loading-based indicator, and the loss-duty curve is proportional to squared loading. Both improve when HNF-ROLM lowers source duty, but neither substitute for AC power flow. Their purpose is to show the expected direction and timing of improvement and to identify the hours that must be re-evaluated once verified line, transformer, tap, and reactive-power data are supplied.

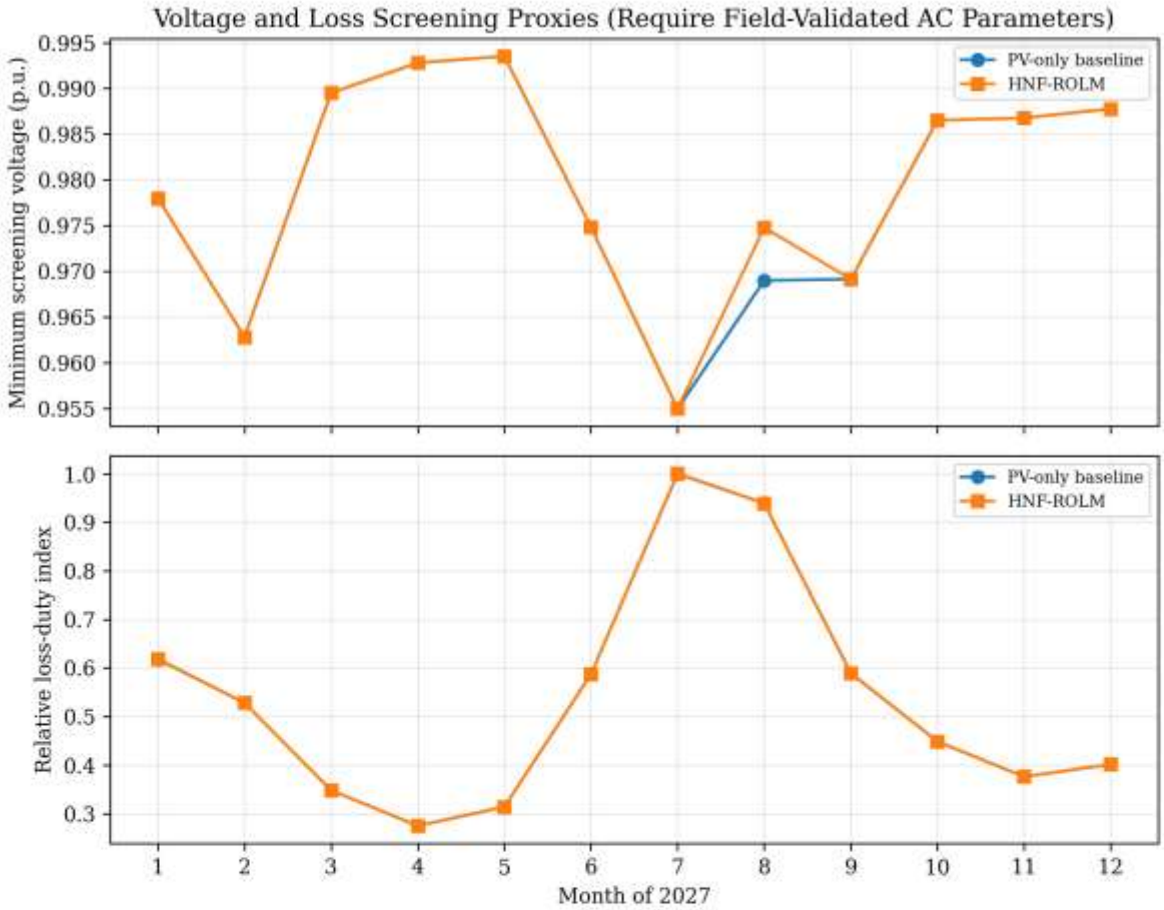

Fig. 17. Voltage and loss-duty screening proxies before and after coordination; complete AC parameters are required for design conclusions.

The voltage and loss curves indicate direction and timing only. Final limits require verified AC power flow and, where relevant, dynamic simulation.

These curves represent chronological operating points, not sub-second transient simulations. A defensible dynamic study must model frequency, voltage, active and reactive power, current, inverter and BESS controls, protection, governors, excitation systems, communication delay, and dynamic loads at an appropriate time step. RMS or electromagnetic-transient claims therefore lie outside the evidence available from the present one-line diagram.

9. ENGINEERING DISCUSSION

The strongest feature of the study is its explicit connection between forecasting and service. The FFNN is not treated as the final product. Its output is compared with a physical envelope, translated into a dispatch action, and then judged by the energy and interruption consequences of that action. This makes the analysis more useful to an operator or planner than a table of forecast errors alone.

The compact network is appropriate to the disclosed sample size, and the chronological holdout reduces the optimism that often accompanies random splitting. Nevertheless, 456 hours from selected reports do not represent a continuous year. Extreme temperature, Ramadan and official-holiday behaviour, switching changes, outages, economic growth, behind-the-meter PV, tariff response, and long-term concept drift may alter the load shape. Rolling validation with continuous Al-Ruwais SCADA, weather, and calendar data is therefore an essential next step.

The ten-year projection explains why an apparently comfortable first-year margin cannot be extrapolated indefinitely. Compound growth consumes normal headroom, and the fixed initial N-1 limit is already inadequate during many high-load conditions. BESS and DR are effective for short-duration risk; they do not create unlimited transfer capability. Their value depends on SOC, sustained duration, customer availability, rebound, communications, degradation, and the probability that PV reduction coincides with an equipment outage.

The resilience indicators must also be interpreted carefully. ENS is directly tied to energy service. SAIDI and SAIFI are conventional customer indices, but the present values are load-weighted planning proxies because customer allocation and event records are unavailable. RI is a study-specific composite, not a universal standard. Its weights and normalization constants should be recalibrated against GECOL policy, critical-load priorities, and historical interruption performance before regulatory use.

Voltage, current, and loss results are likewise conditional on the model. GECOL should confirm line R/X data, conductor ampacity, transformer impedance and taps, phase allocation, switching status, station power factor, reactive demand, protection settings, BESS and inverter capability curves, and actual DR contracts. The final model should be benchmarked against measured pre- and post-disturbance events. Both code versions are structured so verified inputs can be introduced without changing the central HNF-ROLM logic.

As a paper extracted from the doctoral proposal, this work establishes a reproducible case-study foundation rather than claiming completion of the thesis. It demonstrates the research idea in an auditable form: the forecast is linked to a decision, the decision is evaluated through service-oriented indicators, and reinforcement is triggered when operational flexibility is no longer sufficient. After local calibration, the workflow can be transferred to other western-Libyan networks.

10. CONCLUSION

This study developed a ten-year, data-linked planning and operational framework for the Al-Ruwais high-voltage network using 456 hourly observations from 19 GECOL reports, a compact FFNN, and the proposed HNF-ROLM algorithm. MATLAB was retained as the primary implementation, with Python used as an independent verification path. The chronological holdout used 288 earlier observations for training and 168 later observations for testing and produced an MAE of 115.938 MW, an RMSE of 149.938 MW, and a MAPE of 2.944%. These results confirm that the compact model reproduced the main temporal load pattern with useful accuracy, while the residual analysis showed that peak and ramp underprediction must still be covered by an operational reserve.

Coordinated PV+BESS+DR operation achieved the best first-year performance, reducing peak demand from 97.978 MW to 89.831 MW, ENS from 271.1 MWh to 126.6 MWh, SAIDI from 2.837 h to 1.339 h, and SAIFI from 0.421 to 0.345, while increasing RI from 0.892 to 0.939. Over the ten-year horizon, peak demand is projected to reach 195.858 MW, requiring additional transfer capacity in 2030 and 2035. HNF-ROLM also reduced 2036 ENS from 136.0 MWh to 30.7 MWh and improved RI from 0.968 to 0.990. However, the transformer N−1 condition remains the main limitation, confirming that BESS and DR support short-term resilience but cannot replace permanent network reinforcement.

Within these limitations, the study demonstrates the principal contribution of HNF-ROLM: it converts a forecast into a traceable sequence of PV, BESS, DR, transfer, reinforcement, and controlled-shedding decisions, then evaluates the service consequence through ENS, SAIDI, SAIFI, violation hours, and RI. The framework therefore provides a defensible basis for hourly decision support, annual model recalibration, long-term investment timing, and contingency planning in Al-Ruwais and comparable western-Libyan power networks.

REFERENCES

[1] M. K. A. Al-Mashakwi, "Enhancing Electrical Network Resilience through Advanced Load Demand Management, Including Load Forecasting with Renewable Energy Integration in West Libya," Ph.D. research proposal, School of Applied Sciences and Engineering, Libyan Academy for Postgraduate Studies, Libya, 2025, unpublished.

[2] Y. Zhou, D. Qin, and Y. Wang, Shall We Evaluate Load Forecasts," Power and Energy Future, vol. 1, no. 1, Art. no. 9650004, 2026, doi: 10.26599/PEF.2026.9650004.

[3] S. Haykin, Neural Networks and Learning Machines, 3rd ed. Upper Saddle River, NJ, USA: Pearson, 2009.

[4] F. Alhaj Omar and N. Pamuk, "Comparative Forecasting of Electricity Load and Generation in Türkiye Using Prophet, XGBoost, and Deep Neural Networks," Sustainability, vol. 18, no. 6, Art. no. 2838, 2026, doi: 10.3390/su18062838.

[5] J. Eckhoff, S. Wadhwa, M. Fette, J. P. Wulfsberg, and C. Wanigasekara, "Electrical Load Forecasting in the Industrial Sector: A Literature Review of Machine Learning Models and Architectures for Grid Planning," Energies, vol. 19, no. 2, Art. no. 538, 2026, doi: 10.3390/en19020538.

[6] D. Rabie, M. Moradi, W. Xuan, and H. Farzaneh, "Impact of Accurate Load Forecasting on Electricity Market Stability in Japan Using Classical Time-Series and Deep-Learning Methods," Scientific Reports, vol. 16, Art. no. 11781, 2026, doi: 10.1038/s41598-026-46859-2.

[7] H. Liu, Y. Wei, H. Zhang, Y. Wang, J. Zhang, and Z. Luo, "A Hybrid LSTM-Transformer Model for Short-Term Urban Electricity Load Forecasting: A Two-City Case Study," Scientific Reports, vol. 16, Art. no. 16964, 2026, doi: 10.1038/s41598-026-47905-9.

[8] M. Haggag, K. Abdelhady, M. Guirguis, M. Saudy, and W. El Dakhakhni, "Machine Learning Long-Term Electricity Demand Forecasting System for Strategic Energy Investments," Scientific Reports, vol. 16, Art. no. 12471, 2026, doi: 10.1038/s41598-026-45123-x.

[9] S. Luo, X. Chen, X. Pang, B. Wang, and Z. Zheng, "Mid-Term Power Load Forecasting Using an Ensemble Deep Learning Model with BKA and CWGAN-GP Enhancements," Scientific Reports, vol. 16, Art. no. 18612, 2026, doi: 10.1038/s41598-026-49674-x.

[10] K. L. Yandar, O. Revelo Sánchez, and M. Bolaños Gonzales, "Joint Forecasting of Energy Consumption and Generation in P2P Networks Using LSTM-CNN and Transformers," Energies, vol. 19, no. 3, Art. no. 760, 2026, doi: 10.3390/en19030760.

[11] General Electricity Company of Libya (GECOL), General Control Center/Western Region, "Daily Generation, Demand, Frequency, and Load-Shedding Operational Reports," 19 macro-enabled workbooks, unpublished utility operational data, 2023.

[12] M. K. Al-Mashakwi, M. A. Nasrst, and O. M. Abdulrahman, "Analysis of Load Growth and Renewable Energy-Based Optimization of a Libyan Power Network Segment Using ETAP," research manuscript, Az-Zawiya University, Libya, 2026, unpublished.

[13] F. E. Abrahamsen, I. Norheim, and K. O. Uhlen, "Flexibility and Controllability in Low-Voltage Distribution Grids Under High PV Penetration," Energies, vol. 19, no. 9, Art. no. 2072, 2026, doi: 10.3390/en19092072.

[14] R. Mu, Y. Zhang, Y. Wu, X. Wan, X. Song, D. Wang, L. Sun, and B. Yang, "A Critical Review of State-of-the-Art Stability Control of PV Systems: Methodologies, Challenges, and Perspectives," Energies, vol. 19, no. 2, Art. no. 507, 2026, doi: 10.3390/en19020507.

[15] Y. Xu, Z. You, Y. Shi, G. Wang, Y. Wang, and B. Yang, "Optimal Dispatch of Energy Storage Systems in Flexible Distribution Networks Considering Demand Response," Energies, vol. 19, no. 2, Art. no. 407, 2026, doi: 10.3390/en19020407.

[16] H. Saadat, Power System Analysis. Boston, MA, USA: WCB/McGraw-Hill, 1999.

[17] Y. Yang, R. Ou, W. Liu, D. Zheng, K. Hou, C. Wu, Y. Tuo, J. Wang, and J. Tang, "Optimal Operation of Coordinated Transmission and Distribution Networks Considering Multi-Type Flexible Resource Aggregation," Frontiers in Energy Research, vol. 14, Art. no. 1656716, 2026, doi: 10.3389/fenrg.2026.1656716.

[18] MathWorks, "MATLAB Documentation: Language Fundamentals, Optimization, and Neural-Network Implementation Resources," Natick, MA, USA, accessed Jul. 19, 2026.